Inorg. Chem. **2005**, *44*, 7431–7442

Structural and Spectroscopic Study of Reactions between Chelating Zinc-Binding Groups and Mimics of the Matrix Metalloproteinase and Disintegrin Metalloprotease Catalytic Sites: The Coordination Chemistry of Metalloprotease Inhibition

Hongshan He,[†] David T. Puerta,[‡] Seth M. Cohen,[‡] and Kenton R. Rodgers*,[†]

Department of Chemistry, Biochemistry, and Molecular Biology, North Dakota State University, Fargo, North Dakota 58105-5516, and Department of Chemistry and Biochemistry, University of California, San Diego, La Jolla, California 92093-0358

Received May 9, 2005

To understand the coordination chemistry of zinc-binding groups (ZBGs) with catalytic zinc centers in matrix metalloproteinases (MMPs) and disintegrin metalloproteases (ADAMs), we have undertaken a model compound study centered around tris(3,5-methylphenypyrazolyl)hydroboratozinc(II) hydroxide and aqua complexes ([$Tp^{Ph,Me}$-ZnOH] and [$Tp^{Ph,Me}Zn(OH_2)]^+$, respectively, wherein $(Tp^{Ph,Me})^-$ = hydrotris(3,5-methylphenylpyrazolyl)borate) and the products of their reactions with a class of chelating Schiff's base ligands. The results show that the protic ligands, HL (HL = *N*-propyl-1-(5-methyl-2-imidazolyl)methanimine (5-Me-4-ImHPr), *N*-propyl-1-(4-imidazolyl)-methanimine (4-ImHPr), and *N*-propyl-1-(2-imidazolyl)methanimine (2-ImHPr)), react with [$Tp^{Ph,Me}$ZnOH] and give products with the general formula [$Tp^{Ph,Me}$ZnL], whereas reactions with neutral aprotic ligands, L′ (L′ = *N*-propyl-1-(1-methyl-2-imidazolyl)methanimine (1-Me-2-ImPr) and *N*-propyl-1-(2-thiazolyl)methanimine (2-TaPr)), yield the corresponding [$Tp^{Ph,Me}$ZnL]$^+$ complexes. Although the phenol group of *N*-propyl-1-(2-hydroxyphenyl)methanimine (2-HOPhPr) is protic, this ligand forms a cationic four-coordinate complex containing an intraligand hydrogen bond. The solid-state structures of these complexes were determined by single-crystal X-ray diffraction, and the results showed that the protic ligands form five-membered chelates of the Zn^{2+} ion. All ligands displace the aqua ligand in [$Tp^{Ph,Me}Zn(OH_2)]^+$ to yield complexes having ^{1}H NMR spectra consistent with the formation of five membered chelates. The ^{1}H resonance frequencies of the chelating ligands typically shift upfield upon coordination to the zinc center, due to ring current effects from the pendant phenyl groups of the $(Tp^{Ph,Me})^-$ ligand. Thus, the ^{1}H NMR spectra provide a convenient and sensitive means of tracking the solution reactions by titration. The resulting series of spectra showed that the stabilities of the chelates in solution depend on the propensity of the ligands to deprotonate upon chelation of the zinc center. The behaviors of these bidentate ZBGs provide insight into the structural and electronic factors that contribute to the stabilities of inhibited MMPs and ADAMs and suggest that the proton acidity of the coordinated ZBG may be a crucial criterion for inhibitor design.

Introduction

The matrix metalloproteinases (MMPs) and disintegrin metalloproteases (ADAMs) are excreted zinc-dependent endopeptidases that have as their substrates virtually all macromolecular components of the extracellular matrix and many cell surface proteins important to cell−cell communication.[1−7] High sequence homologies (40−50%) are found within the MMPs and ADAMs, which comprise multiple

* To whom correspondence should be addressed. Phone: 701-231-8746. Fax: 701-231-8831. E-mail: kent.rodgers@ndsu.edu.
[†] North Dakota State University.
[‡] University of California, San Diego.

(1) Parkin, G. *Chem. Commun.* **2000**, 1971−1985.
(2) Parkin, G. *Chem. Rev.* **2004**, *104*, 699−767.
(3) Whittaker, M.; Floyd, C. D.; Brown, P.; Gearing, A. J. H. *Chem. Rev.* **1999**, *99*, 2735−2776.
(4) Tsuruda, T.; Costello-Boerrigter, L. C.; Burnett, J. C., Jr. *Heart Failure Rev.* **2004**, *9*, 53−61.
(5) Peterson, J. T. *Heart Failure Rev.* **2004**, *9*, 63−79.
(6) Janicki, J. S.; Brower, G. L.; Gardner, J. D.; Chancey, A. L.; Stewart, J. A. Jr. *Heart Failure Rev.* **2004**, *9*, 33−42.
(7) Kimura, E. *Acc. Chem. Res.* **2001**, *34*, 171−179.

10.1021/ic050723p CCC: $30.25
Published on Web 09/08/2005

domains with largely conserved domain structures.[8−26] The *in vivo* activities of these enzymes are regulated transcriptionally, by posttranslational removal of a prodomain and by interaction with inhibitory proteins called tissue inhibitors of metalloproteinases (TIMPs), which bind to the catalytic domain and block access of substrates to the active sites. Misregulations of these enzyme activities are implicated in a wide variety of tissue degenerative disorders including cancers, arthritis, heart disease, stroke, diabetes, asthma, adipogenesis, and others.[3−7] Consequently, inhibition of these enzymes by pharmaceutical agents is an intensely pursued strategy for exogenous control over abhorrent activity. The vast majority of pharmaceutical inhibition strategies have been based on the TIMP mechanism of inhibition: namely, binding of small molecules to the active site by coordinating to the catalytic zinc center. The enzyme specificity and the stability of the inhibited enzymes have been optimized by designing inhibitors that maximize the number of nonbonded contacts between the inhibitor and the amino acids in the enzyme active sites.[3,27,28] Despite successes in the design and synthesis of potent inhibitors and moderate success in achieving enzyme specificity, virtually none of the most potent metalloproteinase inhibitors (MPIs) have achieved clinical success.[1−7] Poor clinical performance has been attributed in part to poor bioavailability of the inhibitors.[4−6] This is due to short *in vivo* half-lives of the hydroxamic acid zinc-binding group (ZBG) that is most often used in these compounds.[3,29] Thus, clinical success of small-molecule metalloprotease inhibitors will likely hinge, at least in part, on the design of new, more stable ZBGs and their incorporation into candidate drugs.

The zinc-containing catalytic domains exhibit remarkable structural similarity among the MMPs and ADAMs. The catalytic domains generally contain two zinc centers, one that is thought to be responsible for stabilizing the enzyme structure (structural zinc) and another that plays a prominent role in catalysis (catalytic zinc).[1−3] Structural studies based on single-crystal X-ray diffraction and solution NMR spectroscopy have shown that the catalytic Zn^{2+} is uniformly coordinated by three nitrogen atoms from the imidazole side chains of three highly conserved His residues. These protein-based ligands occur in a conserved HEXXHXXGXXH zinc-binding sequence. In addition, the activated enzymes have between one and three water molecules coordinated to the catalytic zinc center.[12]

While the efficacy and mode of inhibition for a synthetic MPI can be quantified by the measurement of its K_i or IC_{50}, these constants do not provide clear insight into the structural basis of effective inhibition.[3] One approach to gaining such insight is to correlate structural properties of the inhibited active site and/or model complexes that mimic the inhibited active site with the extent of enzyme inhibition by the MPI. The structures and reactivities of model complexes are readily investigated by a variety of physical and chemical methods. A number of four-coordinate zinc model complexes have been reported as structural mimics of the $[Zn(His)_3]^{2+}$ moieties of metalloproteinases and carbonic anhydrase. Their hydroxide and/or aqua complexes have been shown to react with substrates and inhibitors to mimic the chemistry and structures of active site complexes.[30−56] A recent model

(8) Nagase, H.; Woessner, J. F., Jr. *J. Biol. Chem.* **1999**, *274*, 21491−21494.
(9) Gall, A.; Ruff, M.; Rama, K. R.; Cuniasse, P.; Yiotakis, A.; Dive, V.; Rio, M.; Basset, P.; Moras1, D. *J. Mol. Biol.* **2000**, *307*, 577−586.
(10) Nar, H.; Werle, K.; Bauer, M. M. T.; Dollinger, H.; Jung, B. *J. Mol. Biol*. **2001**, *312*, 743−751.
(11) Rupert, L. R.; Andreas, K. A.; Braun, M.; Tschesche, H.; Huber, R.; Bode, W.; Maskos, K. *J. Mol. Biol*. **2001**, *312*, 731−742.
(12) Bertini, I.; Calderone, V.; Fragai, M.; Luchinat, C.; Mangani, S.; Terni, B. *Angew. Chem., Int. Ed.* **2003**, *42*, 2673−2676.
(13) Botos, I.; Meyer, E.; Swanson, S. M.; Lemaître V.; Yves E. Y.; Meyer, E. F. *J. Mol. Biol*. **1999**, *292*, 837−844.
(14) Zhang, X.; Gonnella, N. C.; Koehn, J.; Pathak, N.; Ganu, V.; Melton, R.; Parker, D.; Hu, S. I.; Nam, K. Y. *J. Mol. Biol*. **2000**, *301*, 513−524.
(15) Moy, F. J.; Chanda, P. K.; Chen, J. M.; Cosmi, S.; Edris, W.;. Levin, J. I.; Powers, R. *J. Mol. Biol*. **2000**, *302*, 671−689.
(16) Lang, R.; Braun, M.; Sounni, N. E.; Noel, A.; Frankenne, F.; Foidart, J. M.; Bode, W.; Maskos, K. *J. Mol. Biol*. **2004**, *336*, 213−225.
(17) Gong, W.; Zhu, X.; Liu, S.; Teng, M.; Niu, L. *J. Mol. Biol*. **1998**, *283*, 657−668. Pavlovsky, A. G.; Williams, M. G.; Ye, Q. Z.; Ortwine, D. F.; Purchase, C. F., II; White, A. D.; Dhanaraj, V.; Roth, B. D.; Johnson, L. L.; Donald, H. D.; Humblet, C.; Blundell, T. *Protein Sci.* **1999**, *8*, 1455−1462.
(18) Almstead, N. G.; Bradley, R. S.; Pikul, S.; De, B.; Natchus, M. G.; Taiwo, Y. O.; Gu, F.; Williams, L. E.; Hynd, B. A.; Janusz, M. J.; Dunaway, C. M.; Mieling, G. E. *J. Med. Chem.* **1999**, *42*, 4547−4562.
(19) Cheng, M.; De, B.; Almstead, N. G.; Pikul, S.; Dowty, M. E.; Dietsch, C. R.; Dunaway, C. M.; Gu, F.; Hsieh, L. C.; Janusz, M. J.; Taiwo, Y. O.; Natchus. M. G. *J. Med. Chem.* **1999**, *42*, 5426−5436.
(20) Cheng, M.; De, B.; Pikul, S.; Almstead, N. G.; Natchus, M. G.; Anastasio, M. V.; McPhail, S. J.; Snider, C. E.; Taiwo, Y. O.; Chen, L.; Dunaway, C. M.; Gu, F.; Dowty, M. E.; Mieling, G. E.; Janusz, M. J.; Wang-Weigand, S. *J. Med. Chem.* **2000**, *43*, 369−380.
(21) Pikul, S.; Dunham, K. M.; Almstead, N. G.; De, B.; Natchus, M. G.; Taiwo, Y. O.; Williams, L. E.; Hynd, B. A.; Hsieh, L. C.; Janusz, M. J. Gu, F.; Mieling, G. E. *Bioorg. Med. Chem. Lett*. **2001**, *11*, 1009−1013.
(22) Natchus, M. G.; Bookland, R. G.; De, B.; Almstead, N. G.; Pikul, S.; Janusz, M. J.; Heitmeyer, S. A.; Hookfin, E. B.; Hsieh, L. C.; Dowty, M. E.; Dietsch, C. R.; Patel, V. S.; Garver, S. M.; Gu, F.; Pokross, M. E.; Mieling, G. E.; Baker, T. R.; Foltz, D. J.; Peng, S. X.; Bornes, D. M.; Strojnowski, M. J.; Taiwo, Y. O. *J. Med. Chem.* **2000**, *43*, 4948−4963.
(23) Natchus, M. G.; Bookland, R. G.; Laufersweiler, M. J.; Pikul, S.; Almstead, N. G.; De, B.; Janusz, M. J.; Hsieh, L. C.; Gu, F.; Pokross, M. E.; Patel, V. S.; Garver, S. M.; Peng, S. X.; Branch, T. M.; King, S. L.; Baker, T. R.; Foltz, D. J.; Mieling, G. E. *J. Med. Chem.* **2001**, *44*, 1060−1071.
(24) Finzel, B. C.; Baldwin, E. T.; Bryant, G. L., Jr.; Hess, G. F.; Wilks, J. W.; Trepod, C. M.; Mott, J. E.; Marsgall, V. P.; Petzold, G. L.; Poorman, R. A.; O'sullivan, T. J.; Schostarez, H. J.; Mitchell, M. A. *Protein Sci.* **1998**, *7*, 2118−2126.
(25) Browner, M. F.; Smith, W. W.; Castelhanol, A. L. *Biochemistry* **1995**, *34*, 6602−6610.
(26) Tripp, B. C.; Smith, K.; Ferry, J. G. *J. Biol. Chem.* **2001**, *276*, 48615−48618.
(27) Levin, J. I. *Curr. Top. Med. Chem.* **2004**, *4*, 1289−1310.
(28) Rush, T. S., III; Powders, R. *Curr. Top. Med. Chem.* **2004**, *4*, 1311−1327.
(29) Knebel, N. G.; Sharp, S. R.; Madigan, M. J. *J. Chromatogr., B* **1995**, *673*, 213−222.
(30) Puerta, D. T.; Cohen, S. M. *Inorg. Chem.* **2002**, *41*, 5075−5082.
(31) Puerta, D. T.; Cohen, S. M. *Inorg. Chem. Acta* **2002**, *237*, 459−462.
(32) Jacobsen, F. E.; Cohen, S. M. *Inorg. Chem.* **2004**, *43*, 3038−3047.
(33) Puerta, D. T.; Schames, J. R.; Henchman, R. H.; McCammon, J. A.; Cohen, S. M. *Angew. Chem., Int. Ed.* **2003**, *42*, 3772−3774.
(34) Puerta, D. T.; Cohen, S. M. *Inorg. Chem.* **2003**, *42*, 3423−3430.
(35) Puerta, D. T.; Lewis, J. A.; Cohen, S. M. *J. Am. Chem. Soc.* **2004**, *126*, 8388−8389.
(36) Boerzel, H.; Koeckert, M.; Bu, W.; Spingler, B.; Lippard. S. J. *Inorg. Chem.* **2003**, *42*, 1604−1615.
(37) Ruf, M.; Vahrenkamp, H. *Inorg. Chem.* **1996**, *35*, 6571−6578.
(38) Ruf. M.; Weiss, K.; Vehrenkamp, H. *J. Am. Chem. Soc.* **1996**, *118*, 9288−9294.

compound study revealed a clear correlation between the extent of MMP inhibition by a ZBG and the ligand exchange free energy for the displacement of acetohydroxamic acetate (AHA^-) shown in eq 1.[35] This result provides compelling

$$[Tp^{Ph,Me}Zn(AHA)] + HZBG \rightleftharpoons [Tp^{Ph,Me}Zn(ZBG)] + HAHA \quad (1)$$

evidence that, regardless of the number or strengths of nonbonded interactions between the MPI and the enzyme, more strongly binding ZBGs are expected to yield more potent MPIs. Previously, we reported the inhibition of MMP-13 by tris(2-aminoethyl)amine-based tripodal ligands,[57,58] which led us to suggest these ligands as potentially useful zinc-binding platforms for the design of new MMP and ADAM inhibitors. Molecular mechanics-based docking and density functional theory (DFT) calculations[57,59] support the hypothesis that the observed competitive inhibition involves chelation of the catalytic $[Zn(His)_3]^{2+}$ center by one of the three bidentate diimine moieties of the tripodal ligands.

In this study, we explore the properties of simple diimine ZBGs as a class of alternative N_2-based ZBGs. Toward this end, we have prepared a number of bidentate Schiff's base ligands and investigated their interactions with model complexes that mimic the structure of the catalytic zinc centers of the MMPs and ADAMs. This report presents the solid-state and solution characterization of complexes formed by reacting these bidentate ligands (Scheme 1) with the active site model complex, [Tp^{Ph,Me}ZnOH]. Single-crystal X-ray structures show that these ligands form neutral bidentate complexes. Furthermore, solution NMR spectra reveal a stepwise mechanism for conversion of [Tp^{Ph,Me}ZnOH] to the five-coordinate chelates observed in the crystal structures.

Scheme 1

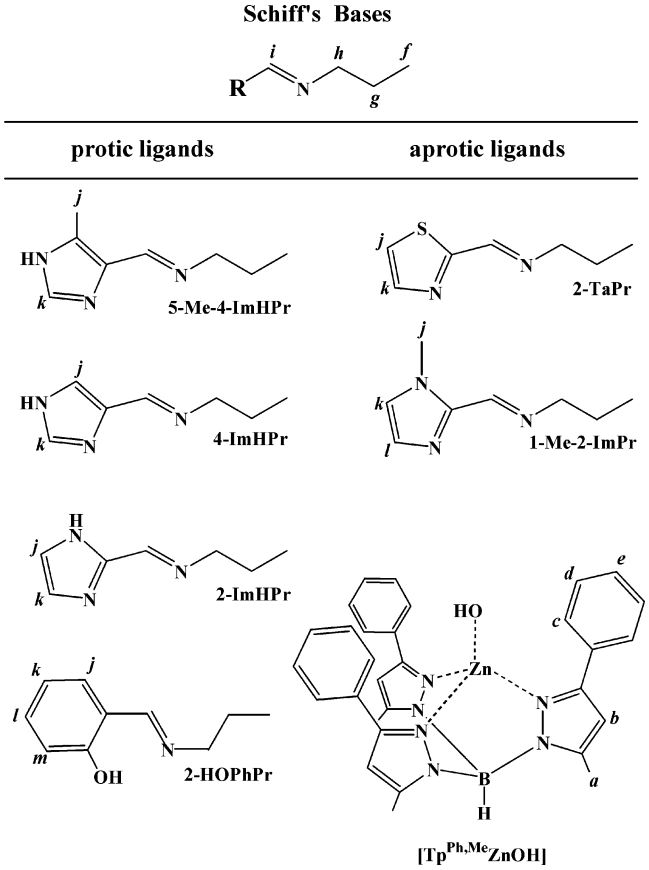

Experimental Methods

Synthetic Procedures. All solvents were treated by standard methods prior to use. Reagent grade 4-methyl-5-imidazolecarboxaldehyde, 1-methyl-2-imidazolecarboxaldehyde, 4-imidazolecarboxaldehyde, 2-imidazolecarboxaldehyde, 2-salicylaldehyde, and *n*-propylamine were obtained commercially and used without further purification. The other chemicals were analytical grade and used as received. [Tp^{Ph,Me}ZnOH] was prepared according to published protocols.[30] Elemental analyses were carried out by a commercial analytical service or using an in-house commercial C, H, and N analyzer. IR spectra were recorded from KBr pellets using a commercial Fourier transform infrared (FT-IR) spectrometer. High-resolution mass spectra were recorded on a commercial time-of-flight instrument. Room temperature (25 °C) ^{1}H and ^{13}C NMR spectra were recorded at 400 or 500 MHz in CD_3OD or $CDCl_3$ solution.

Caution: *Perchlorate salts of compounds containing organic ligands are potentially explosive especially when heated or bumped. Only small amounts of these compounds should be prepared and handled behind suitable protective shields.*

(A) *N*-Propyl-1-(5-methyl-2-imidazolyl)methanimine (5-Me-4-ImHPr). A solution of 4-methyl-5-imidazolecarboxaldehyde (0.99 g, 9 mmol) dissolved in 5 mL of dried methanol was added to a magnetically stirred solution of *n*-propylamine (0.53 g, 9 mmol) in 15 mL of freshly dried methanol. The solution was heated and maintained at reflux for 3 h, after which all solvent was removed by rotary evaporation. The orange solid was thrice washed with MeOH/CH_3CN (v/v = 1:25) and further dried under vacuum. Yield: 0.52 g, 37%. IR (KBr, pellets, cm^{-1}): 2955m, 2928w, 2866m, 2656w, 1642s, 1576s, 1456s, 1355s, 1254m, 1106w, 959s, 854m, 815m. HRMS (ESI): calculated for $C_8H_{14}N_3$, 152.1182; found, 152.1125. ^{1}H NMR (CD_3OD, ppm): 8.25 (s, 1H, imino-

(39) Badura, D.; Vahrenkamp, H. *Inorg. Chem.* **2002**, *41*, 6013−6019.
(40) Looney, A.; Han, R., MeNeill, K.; Parkin, G. *J. Am. Chem. Soc.* **1993**, *115*, 4690−4697.
(41) Han, R.; Correll, I. B.; Looney, A.; Parkin, G. *J. Chem. Soc., Chem. Commun.* **1991**, 717−719.
(42) Trofimenko, S.; Calabrese, J. C.; Thompson, J. S. *Inorg. Chem.* **1987**, *26*, 1570−1514.
(43) Alsfasser, R.; Trofimenko, S.; Looney, A.; Parkin, G.; Vahrenkamp, H. *Inorg. Chem.* **1991**, *30*, 4098−4100.
(44) Alsfasser, R.; Ruf, M.; Trofimenko, S.; Vahrenkamp, H. *Chem. Ber.* **1993**, *126*, 703−710.
(45) Looney, A.; Parkin, G.; Alsfasser, R.; Ruf, M.; Vahrenkamp, H. *Angew. Chem., Int. Ed. Engl.* **1992**, *31*, 92−93.
(46) Ruf, M.; Weis, K.; Brasack, I.; Vahrenkamp, H. *Inorg. Chem. Acta* **1996**, *250*, 271−281.
(47) Bergquist, C.; Fillebeen, T.; Morlok, M. M.; Parkin, G. *J. Am. Chem. Soc.* **2003**, *125*, 6189−6199.
(48) Bergquist, C.; Parkin, G. *J. Am. Chem. Soc.* **1999**, *121*, 6322−6323.
(49) Dowling, C. M.; Parkin, G. *Polyhedron* **2001**, *20*, 285−289.
(50) Guo, S.; Ding, E.; Yin, Y.; Yu, K. *Polyhedron* **1998**, *17*, 3841−3849.
(51) Hammes, B. S.; Luo, X.; Carrano, M. W.; Carrano, C. J. *Inorg. Chem. Acta* **2002**, *341*, 33−38.
(52) Brombacher, H.; Vahrenkamp, H. *Inorg. Chem.* **2004**, *43*, 6042−6049.
(53) Brombacher, H.; Vahrenkamp, H. *Inorg. Chem.* **2004**, *43*, 6050−6053.
(54) Brombacher, H.; Vahrenkamp, H. *Inorg. Chem.* **2004**, *43*, 6054−6060.
(55) Bergquist, C.; Parkin, G. *Inorg. Chem.* **1999**, *38*, 422−423.
(56) Bergquist, C.; Storrie, H.; Koutcher, L.; Bridgewater, B. M.; Friesner, R. A.; Parkin, G. *J. Am. Chem. Soc.* **2000**, *122*, 12651−12658.
(57) He, H.; Linder, D. P.; Rodgers, K. R.; Chakraborthi, I.; Arif, A. M. *Inorg. Chem.* **2004**, *43*, 2392−2401.
(58) He, H.; Rodgers, K. R.; Arif, A. M. *J. Inorg. Biochem.* **2004**, *98*, 667−676.
(59) Linder, D. P.; Rodgers, K. R. *J. Phys. Chem. B* **2004**, *108*, 13839−13849.

[i]H), 7.62 (s, 1H, imidazolyl- [k]H), 3.52 (t, J = 1.5 Hz, 2H, methylene- [h]H), 2.51 (s, 3H, methyl- [j]H), 1.68 (m, 2H, methylene- [g]H), 0.95 (t, J = 7.5 Hz, 3H, methyl- [f]H). ^{13}C NMR (CD_3OD, ppm): 10.36, 11.66, 22.89, 105.08, 128.19, 132.78, 147.15, 153.34.

(B) *N*-Propyl-1-(4-imidazolyl)methanimine (4-ImHPr). This compound was prepared by the procedure described above for 5-Me-4-ImHPr. The reaction was carried out with *n*-propylamine (0.59 g, 10 mmol) and 4-imidazolecarboxaldehyde (0.96 g, 10 mmol). Yield: 0.42 g, 31%. IR (KBr, pellets, cm^{-1}): 2964w, 2391w, 2854w, 2815w, 1656vs, 1581w, 1498vs, 1450s, 1427vs, 1376s, 1340s, 1324s, 1298vs, 1213vs, 1139s, 1087vs, 1062s, 979s, 968vs, 923m, 846s, 790s, 758s, 625vs. HRMS (ESI): calculated for $C_7H_{12}N_3$, 138.1026; found, 138.0972. ^{1}H NMR (CD_3OD, ppm): 8.23 (s, 1H, imino- [i]H), 7.75 (d, J = 0.9 Hz, 1H, imidazolyl- [j]H), 7.53 (s, 1H, imidazolyl- [k]H), 3.51 (dt, J_1 = 1.2 Hz, J_2 = 6.9 Hz, 2H, methylene- [h]H), 1.68 (m, 2H, C methylene- [g]H), 0.94 (t, J = 7.8 Hz, 3H, methyl- [f]H). ^{13}C NMR (CD_3OD, ppm): 10.78, 23.78, 62.58, 123.5, 137.14, 154.3, 163.2.

(C) *N*-Propyl-1-(2-imidazolyl)methanimine (2-ImHPr). This compound was prepared by the procedure described for 5-Me-4-ImHPr. The reaction was carried out with *n*-propylamine (0.30 g, 5 mmol) and 2-imidazolecarboxaldehyde (0.48 g, 5 mmol). Yield: 0.6 g, 44%. IR (KBr, pellets, cm^{-1}): 3018w, 2956w, 2927w, 2875w, 2831w, 2769w, 1650vs, 1596w, 1556m, 1456vs, 1444vs, 1386s, 1303m, 1108s, 1051m, 1012m, 995w, 968m, 900m, 777s, 756vs, 713m. HRMS (ESI): calculated for $C_7H_{12}N_3$, 138.1026; found, 138.1030. ^{1}H NMR (CD_3OD, ppm): 8.13 (d, J = 1.2 Hz, 1H, imino- [i]H), 7.13 (s, 2H, imidazolyl- [j]H and [k]H), 3.55 (t, J = 6.4 Hz, 2H, methylene- [h]H), 1.68 (m, 2H, methylene- [g]H), 0.94 (t, J = 7.2 Hz, 3H, methyl- [f]H). ^{13}C NMR (CD_3OD, ppm):10.8, 23.7, 62.6, 119.2, 143.2, 144.7, 151.0.

(D) *N*-Propyl-1-(2-hydroxyphenyl)methanimine (2-HOPhPr). This compound was prepared by the procedure described for 5-Me-4-ImHPr. The reaction was carried out with *n*-propylamine (0.59 g, 10 mmol) and 2-salicylaldehyde (1.22 g, 10 mmol). Yield: 0.82 g, 50%. IR (KBr, pellets, cm^{-1}): 2962w, 2931w, 2875w, 1633vs, 1583m, 1496s, 1461s, 1415m, 1382w, 1338m, 1280s, 1261s, 1209w, 1151s, 1093s, 1032s, 977s, 804vs, 756vs. HRMS (ESI): calculated for $C_{10}H_{14}NO$, 164.1070; found, 164.1153. ^{1}H NMR (CD_3OD, ppm): 8.35 (s, 1H, imino- [i]H), 7.26−7.22 (m, 2H, phenyl- [j]H and [k]H), 6.80−6.73 (m, 2H, phenyl- [l]H and [m]H), 3.50 (dt, J_1 = 0.8 Hz, J_2 = 6.8 Hz, methylene- [h]H), 1.68 (m, 2H, methylene- [g]H), 0.94 (t, J = 7.2 Hz, 3H, methyl- [f]H). ^{13}C NMR (CD_3OD, ppm): 10.71, 23.84, 59.35, 118.34, 131.79, 132.87, 164.04, 165.55.

(E) *N*-Propyl-1-(2-thiazolyl)methanimine (2-TaPr). This compound was prepared by the procedure described for 5-Me-4-ImHPr. The reaction was carried out with *n*-propylamine (0.29 g, 5 mmol) and 2-thiazolecarboxaldehyde (0.56 g, 5 mmol). Yield: 0.60 g, 78%. IR (KBr, pellets, cm^{-1}): 3079w, 2962m, 2931w, 2873w, 2838w, 1641vs, 1490s, 1419m, 1378w, 1338m, 1226s, 1130s, 1056m, 1010m, 970s, 781s, 730s, 626s. HRMS (ESI): calculated for $C_7H_{11}N_2S$, 155.0637; found, 155.0674. ^{1}H NMR (CD_3OD, ppm): 8.44 (t, J = 1 Hz, 1H, imino- [i]H), 7.92 (d, J = 3 Hz, 1H, thiazolyl- [j]H), 7.66 (dd, J_1 = 1 Hz, J_2 = 3 Hz, 2H, thiazole- [l]H), 3.61 (dt, J_1 = 1.5 Hz, J_2 = 6 Hz, 2H, methylene- [h]H), 1.71 (m, 2H, methylene- [g]H), 0.94 (t, J = 7.5 Hz, 3H, methyl- [f]H). ^{13}C NMR (CD_3OD, ppm): 10.91, 23.56, 62.52, 122.27, 143.66, 155.13, 167.24.

(F) *N*-Propyl-1-(1-methyl-2-imidazolyl)methanimine (1-Me-2-ImPr). This compound was prepared by the procedure described for 5-Me-4-ImHPr. The reaction was carried out with *n*-propylamine (0.29 g, 5 mmol) and 1-methyl-2-imdazolecarboxaldehyde (0.56 g, 5 mmol). Yield: 0.60 g, 78%. IR (KBr, pellets, cm^{-1}): 3114w, 2929w, 2873w, 2831w, 1651vs, 1477s, 1438s, 1377s, 1288s, 1149s, 972m, 752m, 708m. HRMS (ESI): calculated for $C_8H_{14}N_3$, 152.1182; found, 152.1237. ^{1}H NMR (CD_3OD, ppm): 8.25 (s, H, imino- [i]H), 7.17 (s, 1H, imidazolyl- [k]H), 7.05 (s, 1H, imidazolyl- [l]H), 3.98 (s, 3H, methyl- [j]H), 3.57 (m, 2H, methylene- [h]H), 1.72 (m, 2H, methylene- [g]H), 0.98 (t, J = 7.5 Hz, 3H, methyl- [f]H). ^{13}C NMR (CD_3OD, ppm): 10.91, 23.96, 34.48, 63.55, 125.26, 127.89, 143.08, 151.85.

(G) [Tp^{Ph,Me}Zn(5-Me-4-ImPr)]. To a magnetically stirred solution of [Tp^{Ph,Me}ZnOH] (0.060 g, 0.106 mmol) in 10 mL of freshly dried methanol was added a 0.24 mol/L methanol solution of 5-Me-4-ImHPr (0.44 mL, 0.106 mmol) slowly over 10 min. The resulting clear solution was further stirred for 1 h. The solvent was reduced to a volume of 5 mL, and a white solid precipitated. The solid was collected by filtration, washed with heptane, and dried under vacuum. Yield: 50 mg, 67.4%. IR (KBr, pellets, cm^{-1}): 3065w, 2960w, 2929w, 2872w, 2846w, 2541m (B−H), 1620vs, 1545s, 1508m, 1437vs, 1417s, 1369s, 1344s, 1274w, 1180vs, 1068vs, 979s, 837m, 764vs, 696vs, 636s. Anal. Found (Calc) for $C_{38}H_{40}BN_9Zn$: C, 62.99 (65.30); H, 5.50 (5.77); N, 17.45 (18.03). ^{1}H NMR ($CDCl_3$, ppm): 7.39 (d, J = 8.0 Hz, 6H, phenyl- [c]H), 7.23 (t, J = 6.5 Hz, 3H, phenyl- [e]H), 7.13 (t, J = 7.5 Hz, 6H, phenyl- [d]H), 6.83 (s, imino- [i]H), 6.19 (s, 3H, pyrazolyl- [b]H), 5.64 (s, 1H, imidazolyl- [k]H), 2.57 (s, 9H, methyl- [a]H), 2.09 (t, J = 7.0 Hz, 2H, methylene- [h]H), 2.05 (s, 3H, imidazolyl- [j]H), 0.33 (m, 2H, methylene- [g]H), 0.23 (t, J = 7.0 Hz, 3H, methyl- [f]H). ^{13}C NMR ($CDCl_3$, ppm): 153.0, 152.6, 146.5, 145.3, 145.3, 142.4, 132.9, 128.4, 128.2, 127.6, 104.6, 56.9, 21.4, 13.2, 12.7, 11.7.

(H) [Tp^{Ph,Me}Zn(4-ImPr)]. This compound was prepared in the same manner as [Tp^{Ph,Me}Zn(5-Me-4-ImPr)]. 0.060 g (0.106 mmol) of [Tp^{Me,Ph} ZnOH] and a 0.22 mol/L methanol solution of 4-ImHPr (0.48 mL, 0.106 mmol) were used. Yield: 40 mg, 56.0%. IR (KBr, pellets, cm^{-1}): 3060w, 2962w, 2929w, 2871w, 2844w, 2547m (B−H), 1625vs, 1544s, 1506m, 1436s, 1415s, 1367s, 1344s, 1249w, 1178vs, 1116s, 1070vs, 979m, 914w, 782s, 763s, 696vs, 659m, 638m. Anal. Found (Calc) for $C_{37}H_{38}BN_9Zn$: C, 64.54 (64.88); H, 5.47 (5.59); N, 18.24 (18.40). ^{1}H NMR ($CDCl_3$, ppm): 7.38 (d, J = 8.0 Hz, 6H, phenyl- [c]H), 7.22 (t, J = 7.0 Hz, 3H, phenyl- [e]H), 7.12 (t, J = 8.0 Hz, 6H, phenyl- [d]H), 7.02 (s, 1H, imidazolyl- [j]H), 6.89 (s, imino- [i]H), 6.20 (s, 3H, pyrazolyl- [b]H), 5.80 (s, 1H, imidazolyl- [k]H), 2.58 (s, 9H, methyl- [a]H), 2.09 (t, J = 8.0 Hz, 2H, methylene- [h]H), 0.35 (m, 2H, methylene- [g]H), 0.22 (t, J = 7.0 Hz, 3H, methyl- [f]H). ^{13}C NMR ($CDCl_3$, ppm): 158.6, 153.6, 153.0, 146.8, 145.5, 135.9, 132.8, 128.5, 127.7, 127.6, 104.7, 56.7, 21.2, 13.2, 11.7.

(I) [Tp^{Me,Ph}Zn(2-ImPr)]. This compound was prepared in the same manner as [Tp^{Ph,Me}Zn(5-Me-4-ImPr)]. 0.056 g (0.099 mmol) of [Tp^{Me,Ph} ZnOH] and a 0.248 mol/L methanol solution of 2-ImHPr (0.4 mL, 0.099 mmol) were used. Yield: 56 mg, 82.6%. IR (KBr, pellets, cm^{-1}): 3129w, 3091w, 3060w, 2964m, 2931w, 2873w, 2543m (B−H), 1639vs, 1544vs, 1508m, 1481m, 1438vs, 1421vs, 1367s, 1342m, 1182vs, 1151m, 1064vs, 979m, 781vs, 763vs, 696vs, 638m. Anal. Found (Calc) for $C_{37}H_{38}BN_9Zn$: C, 63.53 (64.88); H, 5.85 (5.59); N 18.28 (18.40). ^{1}H NMR ($CDCl_3$, ppm): 7.37 (d, J = 7.0 Hz, 6H, phenyl- [c]H), 7.22 (t, J = 7.5 Hz, 3H, phenyl- [e]H), 7.11 (t, J = 7.5 Hz, 6H, phenyl- [d]H), 6.95 (d, J = 10.5 Hz, 1H, imino- [i]H), 6.21 (s, 3H, pyrazolyl- [b]H), 5.49 (s, 1H, imidazolyl- [j]H), 3.48 (s, 1H, imidazolyl- [k]H), 2.59 (s, 9H, methylene- [a]H), 2.15 (t, J = 7.5 Hz, 2H, methylene- [h]H), 0.39 (m, 2H, methylene- [g]H), 0.23 (t, J = 7.5 Hz, 3H, methyl- [f]H). ^{13}C NMR ($CDCl_3$, ppm): 155.3, 153.2, 151.5, 145.5, 132.7, 131.8, 128.5, 128.4, 128.2, 127.6, 104.7, 56.7, 21.3, 13.2, 11.6.

(J) [Tp^{Ph,Me}Zn(2-OPhPr)]. To a magnetically stirred solution of [Tp^{Ph,Me}ZnOH] (14.5 mg, 2.56 × 10^{-2} mmol) dissolved in 3

mL of freshly dried methanol was added a 0.235 mol/L methanol solution of 2-HOPhPr (108 μL, 2.54×10^{-2} mmol) slowly over 10 min. Then, white solid precipitated immediately. The solvent was reduced to a volume of 1 mL, and the solid was collected by filtration. The solid was washed with heptane and dried under vacuum. Yield: 12 mg, 64%. IR (KBr, pellets, cm^{-1}): 3116w, 3058w, 2958m, 2929w, 2871w, 2528m (B−H), 1629vs, 1600m, 1540vs, 1506m, 1469s, 1452s, 1409s, 1346s, 1189vs, 1174vs, 1087s, 1054s, 1029m, 983s, 917w, 781s, 763vs, 698vs, 632m. Anal. Found (Calc) for $C_{40}H_{40}BN_7OZn$: C, 67.32 (67.48); H, 5.76 (5.80); N, 14.11 (13.77). ^{1}H NMR ($CDCl_3$, ppm): 7.76 (d, $J = 8$ Hz, 6H, phenyl- ^{c}H), 7.20 (t, $J = 8$ Hz, 1H, phenyl- ^{k}H), 7.12 (t, $J = 7.5$ Hz, 3H, phenyl- ^{e}H), 7.08 (t, $J = 7.5$ Hz, 6H, phenyl- ^{d}H), 6.94 (s, 1H, imino- ^{i}H), 6.59 (d, $J = 8.0$ Hz, 1H, phenyl- ^{j}H), 6.46 (t, $J = 7$ Hz, 1H, phenyl- ^{l}H), 6.42 (d, $J = 8.5$ Hz, 1H, phenyl- ^{m}H), 6.24 (s, 3H, pyrazolyl- ^{b}H), 2.57 (s, 9H, methyl- ^{a}H), 2.12 (t, $J = 7.5$ Hz, 2H, methylene- ^{h}H), 0.45 (m, 2H, methylene- ^{g}H), 0.16 (t, $J = 7$ Hz, 3H, methyl- ^{f}H). ^{13}C NMR ($CDCl_3$, ppm): 170.1, 169.1, 156.2, 153.1, 145.5, 134.7, 133.1, 128.2, 127.7, 127.5, 123.7, 119.6, 113.0, 104.2, 59.4, 21.4, 13.4, 11.5.

(K) $[Tp^{Ph,Me}Zn(4\text{-}ImHPr)](ClO_4)$. To a magnetically stirred solution of $[Tp^{Ph,Me}ZnOH]$ (49.7 mg, 8.78×10^{-2} mmol) dissolved in 10 mL of freshly dried methanol was added 0.25 mL of a methanolic solution of $HClO_4$ (0.28 mol/L, 6.25×10^{-2} mmol) slowly over 10 min, and then, 4-ImHPr (12.1 mg, 8.78×10^{-2} mmol) was added. The resulting solution was magnetically stirred for 2 h. Then, the solvent was reduced to a volume of ca. 1 mL and diethylester (5 mL) was added. The solid was collected with filter paper and dried under vacuum. Yield: 59.0 mg, 79%. IR (KBr, pellets, cm^{-1}): 3193w, 3143w, 3116w, 2956w, 2931w, 2873w, 2545m (B−H), 1647s, 1544s, 1506m, 1450s, 1436s, 1417m, 1369s, 1346s, 1180vs, 1112vs, 1097vs, 1068vs, 1016m, 982m, 921w, 835w, 769s, 698vs, 623s. Anal. Found (Calc) for $C_{37}H_{39}N_9O_4BClZn$: C, 56.53 (56.58); H, 5.22 (5.00); N, 16.19 (16.05). ^{1}H NMR (CD_3OD, ppm): 7.36 (d, $J = 7.2$ Hz, 6H, phenyl- ^{c}H), 7.27 (t, $J = 7.2$ Hz, 4H, phenyl- ^{e}H and imidazolyl- ^{k}H), 7.19 (s, 1H, imidazolyl- ^{j}H), 7.13 (t, $J = 7.6$ Hz, 6H, phenyl- ^{d}H), 6.33 (s, 3H, pyrazolyl- ^{b}H), 5.80 (s, 1H, imino- ^{i}H), 2.60 (s, 9H, methyl- ^{a}H), 2.25 (t, $J = 8$ Hz, 2H, methylene- ^{h}H), 0.44 (m, 2H, methylene- ^{g}H), 0.31 (t, $J = 7.2$ Hz, 3H, methyl- ^{f}H). ^{13}C NMR (CD_3OD, ppm): 160.8, 153.0, 152.5, 146.7, 136.0, 138.5, 132.9, 128.7, 128.4, 127.4, 104.7, 56.5, 20.3, 11.6, 10.4.

(L) $[Tp^{Ph,Me}Zn(5\text{-}Me\text{-}4\text{-}ImHPr)](ClO_4)$. This compound was prepared in the same manner as $[Tp^{Ph,Me}Zn(4\text{-}ImHPr)](ClO_4)$. $[Tp^{Ph,Me}ZnOH]$ (59.2 mg, 0.10 mmol) and 5-Me-4-ImHPr (15.8 mg, 0.1 mmol) and a $HClO_4$ methanol solution (0.28 M, 0.3 mL) were used. Yield: 50 mg, 59%. IR (KBr, pellets, cm^{-1}): 3147w, 3060w, 2962m, 2929m, 2873w, 2544m (B−H), 1645vs, 1545vs, 1506m, 1438vs, 1417s, 1369s, 1344s, 1176vs, 1106vs, 1070vs, 982s, 919w, 837w, 779s, 764s, 623m. Anal. Found (Calc) for $C_{38}H_{41}N_9O_4BClZn$: C, 57.31 (57.09); H, 5.43 (5.17); N, 16.11 (15.77). ^{1}H NMR (CD_3OD, ppm): 7.36 (td, $J_1 = 2$ Hz, $J_2 = 6.8$ Hz, phenyl- ^{c}H), 7.28 (tt, $J_1 = 1.2$ Hz, $J_2 = 7.6$ Hz, 4H, phenyl- ^{e}H), 7.21 (d, $J_1 = 0.8$ Hz, 1H, imidazole- ^{k}H), 7.60 (t, $J = 7.6$ Hz, 6H, phenyl- ^{d}H), 6.33 (s, 3H, pyrazolyl - ^{b}H), 5.66 (s, 1H, imino- ^{i}H), 2.59 (s, 9H, methyl- ^{a}H), 2.26 (t, $J = 6$ Hz, 2H, methylene- ^{h}H), 0.40 (m, 2H, methylene- ^{g}H), 0.31 (t, $J = 6.8$ Hz, 3H, methyl- ^{f}H). ^{13}C NMR (CD_3OD, ppm): 152.9, 151.7, 149.2, 145.0, 146.4, 138.4, 133.0, 128.6, 128.3, 127.5, 104.7, 56.9, 20.5, 11.6, 10.4, 7.3.

(M) $[Tp^{Ph,Me}Zn(2\text{-}ImHPr)](ClO_4)$. This compound was prepared in the same manner as $[Tp^{Ph,Me}Zn(4\text{-}ImHPr)](ClO_4)$. $[Tp^{Ph,Me}ZnOH]$ (64.7 mg, 0.11 mmol) and 2-ImHPr (15.7 mg, 0.11 mmol) and a $HClO_4$ methanol solution (0.28 M, 0.32 mL) were used. Yield: 61 mg, 68%. IR (KBr, pellets, cm^{-1}): 3135w, 3105w, 3062w, 2966m, 2933m, 2540m (B−H), 1645s, 1544s, 1506m, 1483s, 1452s, 1438s, 1417vs, 1369s, 1340s, 1182vs, 1105vs, 1066vs, 1020m, 981s, 781s, 763s, 696s, 623vs. Anal. Found (Calc) for $C_{37}H_{39}N_9O_4BClZn$: C, 56.21 (56.58); H, 5.24 (5.00); N, 15.84 (16.05). ^{1}H NMR (CD_3OD, ppm): 7.33 (d, $J = 6.8$ Hz, 6H, phenyl- ^{c}H), 7.27 (t, $J = 7.6$ Hz, 1H, phenyl- ^{e}H), 7.22 (d, $J = 1.2$ Hz, 1H, imidazolyl- ^{j}H), 7.16 (t, $J = 7.2$ Hz, 6H, phenyl- ^{d}H), 6.99 (s, 1H, imidazole- ^{k}H), 6.34 (d, $J = 0.8$ Hz, 3H, pyrazolyl- ^{b}H), 5.31 (s, 1H, imino- ^{i}H), 2.60 (s, 9H, methyl- ^{a}H), 2.38 (t, $J = 7.6$ Hz, 2H, methylene- ^{h}H), 0.45 (m, 2H, methylene- ^{g}H), 0.35 (t, $J = 7.6$ Hz, 3H, methyl- ^{f}H). ^{13}C NMR (CD_3OD, ppm): 153.1, 147.0, 146.9, 132.9, 128.8, 128.3, 128.0, 127.8, 127.4, 121.3, 104.8, 57.7, 20.5, 11.6, 10.3.

(N) $[Tp^{Ph,Me}Zn(2\text{-}TaPr)](ClO_4)$. This compound was prepared in the same manner as $[Tp^{Ph,Me}Zn(4\text{-}ImHPr)](ClO_4)$. $[Tp^{Ph,Me}ZnOH]$ (60.0 mg, 0.11 mmol) and 2-TaPr (19.0 mg, 0.11 mmol) and a $HClO_4$ methanol solution (0.28 M, 0.32 mL) were used. Yield: 60 mg, 70.0%. IR (KBr, pellets, cm^{-1}): 3132w, 3114w, 3062w, 3045w, 2968m, 2927m, 2544m (B−H), 1639s, 1543s, 1506m, 1475s, 1438s, 1416s, 1369s, 1338s, 1184vs, 1097vs, 1070vs, 983s, 910w, 829w, 781s, 763s, 623m. Anal. Found (Calc) for $C_{37}H_{38}N_8O_4SBClZn$: C, 55.34 (55.38); H, 4.97 (4.77); N, 14.18 (13.96). ^{1}H NMR (CD_3OD, ppm): 7.89 (br, 1H, thiazolyl- ^{j}H), 7.80 (s, 1H, thiazolyl- ^{k}H), 7.41 (br, 6H, phenyl- ^{c}H), 7.33 (t, $J = 7.5$ Hz, 6H, phenyl- ^{e}H), 7.25 (br, 1H, phenyl- ^{d}H), 6.81 (br, 1H, imino- ^{i}H), 6.38 (s, 3H, pyrazolyl- ^{b}H), 2.88 (br, 2H, methylene- ^{h}H), 2.63 (s, 9H, methyl- ^{a}H), 0.88 (br, 2H, methylene- ^{h}H), 0.56 (s, 3H, methyl- ^{f}H). ^{13}C NMR (CD_3OD, ppm): 153.3, 147.2, 142.6, 132.8, 130.2, 128.9, 128.6, 128.2, 127.4, 105.1, 51.1, 22.9, 11.6, 10.4, 10.3.

(O) $[Tp^{Ph,Me}Zn(1\text{-}Me\text{-}2\text{-}ImHPr)](ClO_4)$. This compound was prepared in the same manner as $[Tp^{Ph,Me}Zn(2\text{-}TaPr)](ClO_4)$. $[Tp^{Ph,Me}ZnOH]$ (61.7 mg, 0.11 mmol), a $HClO_4$ methanol solution (0.35 mL methanol solution, 0.28 M), and 1-Me-2-ImPr (0.33 mL methanol solution, 0.33 M) were used. Yield: 59 mg, 68%. IR (KBr, pellets, cm^{-1}): 3133w, 2966w, 2924w, 2543m (B−H), 1738s, 1638w, 1506m, 1444s, 1176s, 1091vs, 1060vs, 982s, 768s, 691s, 617m, 605m. Anal. Found (Calc) for $C_{38}H_{41}N_9O_4BClZn$: C, 56.73 (57.09); H, 5.24 (5.17); N, 15.84 (15.77). ^{1}H NMR (CD_3OD, ppm): 7.34−7.31 (m, 9H, phenyl- ^{c}H, ^{e}H, and ^{k}H), 7.29 (s, 1H, imidazolyl- ^{l}H), 7.19 (t, $J = 7.6$ Hz, 6H, phenyl- ^{d}H), 6.34 (s, 3H, pyrazolyl- ^{b}H), 5.28 (s, 1H, imino- ^{i}H), 3.52 (s, 1H, imidazolyl *N*-methyl- ^{j}H), 2.60 (s, 9H, methyl- ^{a}H), 2.40 (t, $J = 8.0$ Hz, 2H, methylene- ^{h}H), 0.45 (m, 2H, methylene- ^{g}H), 0.37 (t, $J = 7.2$ Hz, 3H, methyl- ^{f}H). ^{13}C NMR (CD_3OD, ppm): 153.0, 147.3, 146.2, 136.6, 132.9, 128.8, 128.3, 127.8, 127.4, 126.0, 104.8, 58.0, 32.2, 20.5, 11.6, 10.4.

(P) $[Tp^{Ph,Me}Zn(2\text{-}HOPhPr)](ClO_4)$. This compound was prepared in the same manner as $[Tp^{Ph,Me}Zn(2\text{-}TaPr)](ClO_4)$. $[Tp^{Ph,Me}ZnOH]$ (81.2 mg, 0.14 mmol), a $HClO_4$ methanol solution (10 μL $HClO_4$ solution, 70%), and 2-OHPhPr (0.61 mL methanol solution, 0.235 M) were used. Yield: 84 mg, 72%. IR (KBr, pellets, cm^{-1}): 3048m, 2959m, 2854w, 2528m (B−H), 1619s, 1533s, 1475s, 1448s, 1343s, 1168s, 1052s, 982m, 761s, 691s, 636m. ^{1}H NMR ($CDCl_3$, ppm): 7.75 (d, $J = 7$ Hz, 6H, phenyl- ^{c}H), 7.18 (t, $J = 8.5$ Hz, 1H, phenyl- ^{k}H), 7.12−7.05 (m, 9H, phenyl- ^{d}H and ^{e}H), 6.94 (s, 1H, imino- ^{i}H), 6.59 (d, $J = 7.5$ Hz, 1H, phenyl- ^{j}H), 6.45 (t, $J = 7.0$ Hz, 1H, phenyl- ^{l}H), 6.41 (d, $J = 8.5$ Hz, 1H, phenyl- ^{m}H), 6.23 (s, 3H, pyrazolyl- ^{b}H), 2.56 (s, 9H, methyl- ^{a}H), 2.11 (t, $J = 7.5$ Hz, 2H, methylene- ^{h}H), 0.44 (m, 2H, methylene- ^{g}H), 0.15 (t, $J = 7.5$ Hz, 3H, methyl- ^{f}H). ^{13}C NMR ($CDCl_3$, ppm): 169.2, 153.1, 145.5, 134.7, 133.1, 128.6, 128.5, 128.2, 127.7, 127.5, 123.7, 119.6, 113.0, 104.2, 59.4, 21.4, 13.3, 11.4.

NMR Titrations. ^{1}H NMR titrations of $[Tp^{Me,Ph}ZnOH]$ by ligands were carried out at 500 MHz and at 25 °C. The initial

Table 1. X-ray Diffraction Data for [(Tp^{Ph,Me})Zn(5-Me-4-ImPr)]·C_6H_6, [(Tp^{Ph,Me})Zn(2-HOPhPr)](ClO_4), and [(Tp^{Ph,Me})Zn(2-ImPr)]·C_6H_6

	[Tp^{Ph,Me}Zn(5-Me-4-ImPr)]·C_6H_6	[Tp^{Ph,Me}Zn(2-HOPhPr)]ClO_4	[Tp^{Ph,Me}Zn(2-ImPr)]·C_6H_6
emp formula	$C_{44}H_{40}BN_9Zn$	$C_{40}H_{41}BN_7ClO_5Zn$	$C_{43}H_{44}BN_9Zn$
crystal system	triclinic	monoclinic	triclinic
space group	$P\bar{1}$ (No. 2)	$P2_1/c$ (No. 14)	$P\bar{1}$ (No. 2)
unit cell dimensions	a = 12.8473(15) Å b = 13.3709(16) Å c = 13.3952(16) Å α = 102.369(2)° β = 96.125(2)° γ = 115.455(2)°	a = 15.2835(15) Å b = 11.7403(12) Å c = 21.487(2) Å α = 90° β = 101.066(2)° γ = 90°	a = 11.295(3) Å b = 13.197(3) Å c = 13.438(3) Å α = 87.788(4)° β = 73.274(4)° γ = 81.660(4)°
volume (Å^3)	1977.2(4)	3783.8(7)	1898.0(7)
Z	2	4	2
crystal size (mm^3)	0.40 × 0.30 × 0.20	0.30 × 0.10 × 0.05	0.50 × 0.50 × 0.10
temperature (K)	100(1)	100(1)	100(1)
reflns collected	12579	32102	16518
independ reflns	8731 [R(int) = 0.0196]	8656 [R(int) = 0.0449]	8496 [R(int) = 0.0285]
λ (Å)	0.71073	0.71073	0.71073
ρ_{calcd} (g cm^{-3})	1.295	1.424	1.335
μ (mm^{-1})	0.655	0.775	0.692
final R indices $I > 2\sigma(I)$[a]	R_1 = 0.0477 wR2 = 0.1278	R_1 = 0.0452 wR2 = 0.0990	R_1 = 0.0442 wR2 = 0.0986
R indices (all data)[a]	R_1 = 0.0544 wR2 = 0.1328	R_1 = 0.0624 wR2 = 0.1048	R_1 = 0.0591 wR2 = 0.1047

[a] $R_1 = \sum||F_o| - |F_c||/\sum|F_o|$; $R_2 = \{\sum[w(F_o^2 - F_c^2)^2]/\sum(wF_o^4)\}^{1/2}$.

[Tp^{Ph,Me}ZnOH] concentration was ~1.0 × 10^{-2} M, and the titrant solutions were ~0.24 M in the bidentate zinc-binding ligand. The following details are typical of the NMR titration experiments. A 1.025 × 10^{-2} M solution of [Tp^{Ph,Me}ZnOH] in methanol-d_4 (0.8 mL) was treated with aliquots of 0.24 M 5-Me-4-ImHPr in methanol-d_4 using a 10 μL syringe. The resulting solution was kept at 25 °C for 5 min to ensure that equilibrium had been established, and then, the spectra were recorded. The spectral assignments were based on chemical shifts, coupling patterns, integrals, and COSY maps. Chemical shifts were referenced to TMS.

X-ray Crystallographic Analysis. Data were collected on a Bruker diffractometer equipped with an AXS area detector. Crystals were mounted on quartz capillaries by using Paratone oil and were cooled on the diffractometer to ~173 °C in a temperature controlled nitrogen stream. Peak integrations were performed with the Siemens SAINT software package. Absorption corrections were applied using the program SADABS. Space group determinations were performed with the program XPREP. The structures were solved by direct or Patterson methods and refined with the SHELXTL software package.[60] Unless noted otherwise, all hydrogen atoms, except for the boron hydrogen atoms, were fixed at calculated positions with isotropic thermal parameters; all non-hydrogen atoms were refined anisotropically.

(A) Preparation of [Tp^{Ph,Me}Zn(5-Me-4-ImPr)] Single Crystals. In a 100 mL round-bottom flask, [Tp^{Ph,Me}ZnOH] (100 mg, 0.18 mmol) was dissolved in 20 mL of anhydrous CH_2Cl_2. To this solution was added 1.0 equiv of 5-Me-4-ImHPr (26.7 mg, 0.18 mmol) dissolved in 20 mL of anhydrous CH_2Cl_2. The mixture was stirred at room temperature overnight under a nitrogen atmosphere. After stirring, the turbid solution was evaporated to dryness on a rotary evaporator to give a white solid. The solid was dissolved in a minimum volume of benzene (~15 mL) and filtered to remove any insoluble material, and the filtrate was recrystallized by diffusion of pentane into the solution. The yield of crystalline product was 81%. This method yielded colorless blocks suitable for X-ray analysis (Table 1). The hydrogen atom on the boron was found in the difference map, and its position was refined. The complex cocrystallized with one molecule of benzene that was refined in two orientations having 70% and 30% occupancies. No hydrogen atoms were calculated or refined for the disordered benzene solvent molecule. The disordered benzene molecule was not refined anisotropically. Anal. Found (Calc) for $C_{38}H_{40}N_9BZn$·C_6H_6: C, 67.82 (68.01); H, 6.14 (5.97); N, 16.41 (16.22).

(B) Preparation of [Tp^{Ph,Me}Zn(2-ImPr)] Single Crystals. This compound was prepared in 83% yield, as described above for [Tp^{Ph,Me}Zn(5-Me-4-ImPr)]. This method yielded colorless blocks suitable for X-ray analysis (Table 1). The hydrogen atom on the boron was found in the difference map, and its position was refined. The complex cocrystallized with one molecule of benzene in the asymmetric unit. Anal. Found (Calc) for $C_{37}H_{38}N_9BZn$·C_6H_6: C, 67.73 (67.68); H, 5.81 (5.81); N, 16.73 (16.52).

(C) Preparation of [Tp^{Ph,Me}Zn(2-HOPhPr)]ClO_4 Single Crystals. This compound was prepared in 20% yield, as described above. This method yielded yellow plates suitable for X-ray analysis (Table 1). The hydrogen atoms on the boron and imine were found in the difference map, and their positions were refined. The complex cocrystallized with one perchlorate ion in the asymmetric unit.

Results and Discussion

Six bidentate ligands have been synthesized, and their zinc-binding properties have been investigated by reaction with zinc hydridotris(3-methyl-5-phenylpyrazole-1-yl)borate hydroxide ([Tp^{Ph,Me}ZnOH]), which acts as a structural mimic of the MMP and ADAM active sites. These zinc-binding groups and the model complex are shown in Scheme 1. The bidentate ligands can be divided into two groups, protic (HL) and aprotic (L′). The aprotic ligands displace the hydroxide or water ligand from zinc to yield cationic [Tp^{Ph,Me}Zn(L′)]$^+$ complexes, whereas the protic ligands have the possibility to react with the zinc hydroxide complex to produce water and a charge-neutral [Tp^{Ph,Me}Zn(L)] complex.

Single-Crystal X-ray Structures. The structures of the complexes formed upon reaction of [Tp^{Ph,Me}ZnOH] and three of the ligands were determined by single-crystal X-ray diffraction. Table 1 lists the crystallographic parameters for [Tp^{Ph,Me}Zn(5-Me-4-ImPr)]·C_6H_6, [Tp^{Ph,Me}Zn(2-ImPr)]·C_6H_6, and [Tp^{Ph,Me}Zn(2-HOPhPr)]ClO_4. The ORTEP diagram of [Tp^{Ph,Me}Zn(5-Me-4-ImPr)]·C_6H_6 is shown in Figure 1A. The

(60) Sheldrick, G. M. *SHELX97: Programs for Crystal Structure Analysis*, Release 97−2; University of Göttingen: Göttingen, Germany, 1997.

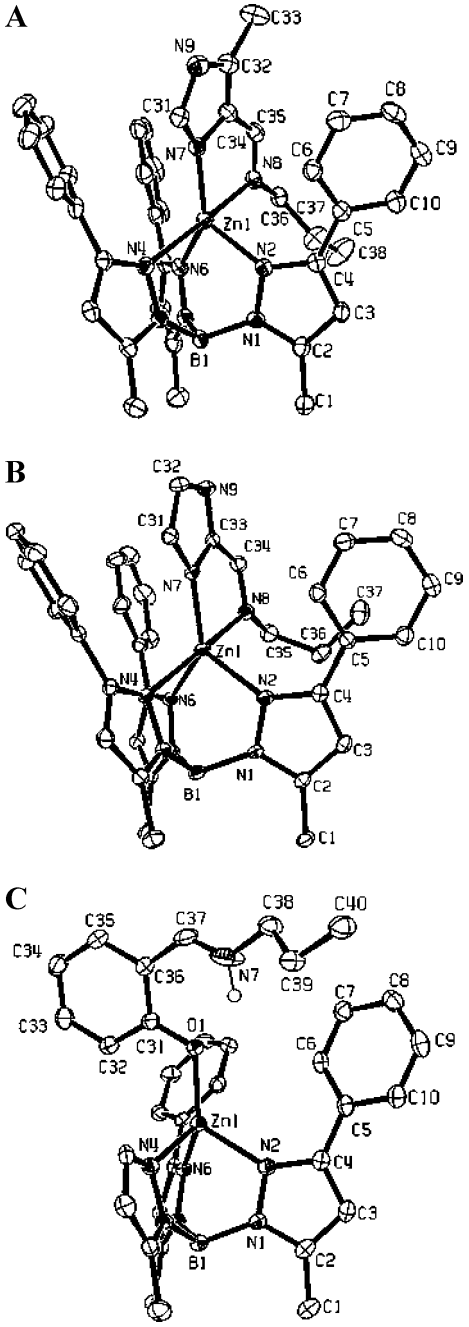

Figure 1. Structural diagrams of (A) [(Tp^{Ph,Me})Zn(5-Me-4-ImPr)]·C_6H_6, (B) [(Tp^{Ph,Me})Zn(2-ImPr)]·C_6H_6, and (C) [(Tp^{Ph,Me})Zn(2-HOPhPr)]ClO_4 with partial atom numbering schemes (ORTEP, 50% probability ellipsoids). Hydrogen atoms, solvent molecules, and counterions have been omitted for clarity.

(5-Me-4-ImPr)$^-$ ligand coordinates to the zinc ion as a bidentate anion to yield a neutral complex. The five-membered chelate ring defined by N(7), N(8), C(34), C(35), and Zn(1) is nearly planar and nearly coplanar with the imidazolyl ring (dihedral angle $\approx 7°$). The geometry of the complex can be described as distorted trigonal pyramid ($\tau = 0.48$) with N(2), N(6), and N(7) defining the equatorial plane, and N(4) and N(8) in the axial positions. The axial Zn$-$N$_{pyrazolyl}$ distance (Table 2) is 0.139 Å shorter than the equatorial distances (mean = 2.071 Å), and the two Zn$-$N$_{ZBG}$ distances are inequivalent, with the Zn$-$N$_{Im}$ distance being 0.223 Å shorter than its Zn$-$N$_{imine}$ counterpart. The

Table 2. Selected Bond Distances (Å) and Angles (deg) for [Tp^{Ph,Me}Zn(5-Me-4-ImPr)]·C_6H_6 and [Tp^{Ph,Me}Zn(2-ImPr)]·C_6H_6

bond	distance	bond	angle
[Tp^{Ph,Me}Zn(5-Me-4-ImPr)]·C_6H_6			
Zn(1)−N(6)	2.0735(19)	N(2)−Zn(1)−N(4)	89.19(7)
Zn(1)−N(2)	2.0703(19)	N(2)−Zn(1)−N(6)	98.90(7)
Zn(1)−N(4)	2.2102(19)	N(6)−Zn(1)−N(4)	80.80(7)
Zn(1)−N(7)	1.9871(19)	N(7)−Zn(1)−N(8)	80.21(7)
Zn(1)−N(8)	2.2147(19)	Zn(1)−N(2)−N(1)	113.16(13)
B(1)−N(1)	1.554(3)	Zn(1)−N(6)−N(5)	114.22(3)
B(1)−N(3)	1.543(3)	Zn(1)−N(4)−N(3)	110.81(13)
B(1)−N(5)	1.546(3)	Zn(1)−N(7)−C(34)	112.94(14)
		Zn(1)−N(8)−C(35)	108.98(15)
[Tp^{Ph,Me}Zn(2-ImPr)]·C_6H_6			
Zn(1)−N(2)	2.0593(18)	N(2)−Zn(1)−N(4)	88.49(7)
Zn(1)−N(4)	2.2482(19)	N(2)−Zn(1)−N(6)	98.53(7)
Zn(1)−N(6)	2.0309(18)	N(6)−Zn(1)−N(4)	81.55(7)
Zn(1)−N(7)	1.9778(18)	N(7)−Zn(1)−N(8)	78.61(7)
Zn(1)−N(8)	2.3179(19)	Zn(1)−N(2)−N(1)	112.79(13)
B(1)−N(1)	1.548(3)	Zn(1)−N(4)−N(3)	109.42(13)
B(1)−N(3)	1.5487(3)	Zn(1)−N(6)−N(5)	116.13(13)
B(1)−N(5)	1.552(3)	Zn(1)−N(7)−C(33)	115.44(15)
		Zn(1)−N(8)−C(34)	106.98(15)

Table 3. Selected Bond Distances (Å) and Angles (deg) for [Tp^{Ph,Me}Zn(2-HOPhPr)]ClO_4

bond	distance	bond	angle
[Tp^{Ph,Me}Zn(2-HOPhPr)]ClO_4			
Zn(1)−N(2)	2.0359(19)	N(2)−Zn(1)−N(4)	94.63(18)
Zn(1)−N(4)	2.0095(19)	N(2)−Zn(1)−N(6)	90.54(7)
Zn(1)−N(6)	2.0268(19)	N(6)−Zn(1)−N(4)	96.26(8)
B(1)−N(3)	1.554(3)	Zn(1)−N(2)−N(1)	111.18(13)
B(1)−N(5)	1.547(3)	Zn(1)−N(4)−N(3)	111.48(14)
B(1)−N(1)	1.555(3)	Zn(1)−N(6)−N(5)	110.25(14)
Zn(1)−O(1)	1.8924(16)	N(2)−Zn(1)−O(1)	123.39(7)
		N(4)−Zn(1)−O(1)	118.10(7)
		N(6)−Zn(1)−O(1)	126(7)

equatorial N−Zn−N angles are 99°, 118°, and 142° with $\angle N_{Pz}-Zn-N_{Pz}$ being the smallest (Table 2). Figure 1B shows the structure of [Tp^{Ph,Me}Zn(2-ImPr)]·C_6H_6, which is a neutral complex with a distorted trigonal bipyramidal structure ($\tau = 0.60$) similar to that of the (5-Me-4-ImPr)$^-$ analogue described above. Although we were unsuccessful in growing diffraction quality crystals of [Tp^{Ph,Me}Zn(4-ImPr)], elemental analysis and ^{1}H NMR data are consistent with a structure analogous to those in Figure 1.

As seen in Figure 1C, the structure of [Tp^{Ph,Me}Zn(2-HOPhPr)](ClO_4) is distinct from those of the imidazole-based ligand complexes. The 2-HOPhPr ligand coordinates to zinc as a neutral monodentate ligand, and the complex carries a single positive charge. Selected bond lengths and angles are listed in Table 3. The phenol proton was located in the Fourier difference map, and its position was refined. This position shows it to have been transferred to the imine N atom (N−H = 0.982 Å), and the imine N and phenol O atoms are H-bonded with a N···H···O distance of 2.672 Å. The Zn−O bond distance of 1.893 Å is typical of a phenolate ligand.[61] Similar intramolecular H-bonding has also been observed for zinc−thiolate complexes.[36] As shown in Figure 1C, the phenol ring and the six-membered ring formed by the H-bond are nearly coplanar. The ClO_4^- counterion does not coordinate to the zinc ion, and the Zn^{2+} is four-coordinate with a distorted tetrahedral geometry.

(61) Huheey, J. E. *Inorganic Chemistry*, 2nd ed.; Harper & Row Publishers: New York, 1978.

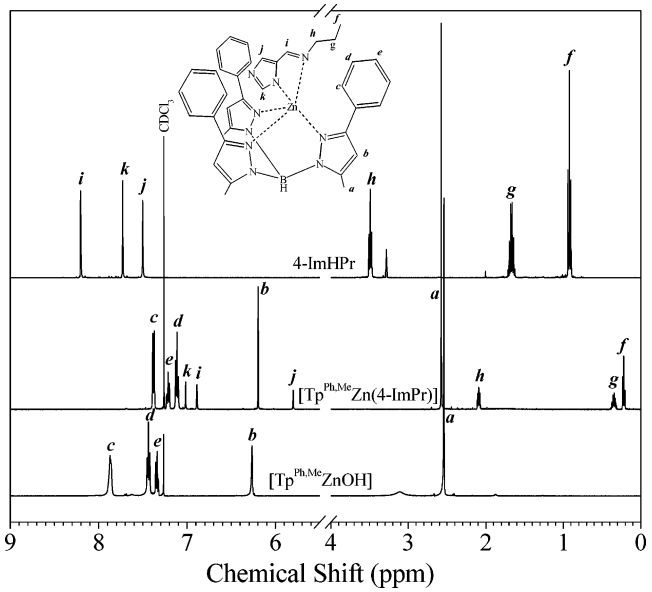

Figure 2. 500 MHz ^{1}H NMR spectra of [$Tp^{Ph,Me}$ZnOH] (in $CDCl_3$, bottom), [$Tp^{Ph,Me}$Zn(4-ImPr)] (in $CDCl_3$, middle), and 4-ImHPr (in CD_3-OD, top) at 25 °C.

^{1}H NMR Spectra of the Complexes. Formation of the complexes was followed by changes in the ^{1}H NMR spectra during titrations of [$Tp^{Ph,Me}$ZnOH] by the six aforementioned ligands. The spectra of the [$Tp^{Ph,Me}$Zn(L)] complexes are distinct from that of [$Tp^{Ph,Me}$ZnOH] due to changes in the chemical shifts of the $(Tp^{Ph,Me})^-$ resonances upon coordination of the bidentate ligands and due to the appearance of their resonances, whose chemical shifts in the [$Tp^{Ph,Me}$Zn(L)] complexes are diagnostic of coordination (*vide infra*). Figure 2 shows the ^{1}H NMR spectra of [$Tp^{Ph,Me}$ZnOH], [$Tp^{Ph,Me}$Zn(4-ImPr)], and 4-ImHPr. The proton resonances of the propyl group in the free 4-ImHPr ligand appear at 0.94, 1.68, and 3.51 ppm for ^{f}H, ^{g}H, and ^{h}H, respectively. The corresponding resonances in the [$Tp^{Ph,Me}$Zn(4-ImPr)] spectrum appear at 0.22, 0.35, and 2.05 ppm. The imine proton (^{i}H) occurs at 8.23 ppm in the free ligand spectrum and at 6.95 ppm in the complex. The imidazole resonances in the free ligand appear at 7.75 and 7.73 ppm for ^{j}H and ^{k}H, respectively. The corresponding resonances in the complex occur at 5.49 and 3.48 ppm. All $(4\text{-ImPr})^-$ resonances in the spectrum of [$Tp^{Ph,Me}$Zn(4-ImPr)] occur upfield of their counterparts in the spectrum of free 4-ImHPr. Absent other factors, coordination of the diimine ligands to zinc would be expected to elicit downfield shifts of their ^{1}H resonances relative to their frequencies in the spectra of the free ligands. Therefore, the upfield shifts are attributed to other effects. Examination of the structures in Figure 1 reveals that all of the ligand protons lie within the shielding zone of one or more 5-phenyl rings from the $[Tp^{Ph,Me}Zn]^+$ moiety. Thus, the upfield changes in the diimine chemical shifts are attributed to intramolecular ring current effects.[62] The 5-phenyl groups of the [$Tp^{Ph,Me}$ZnL] complexes give rise to only three multiplets, suggesting that ortho and meta protons undergo rapid site exchange on the NMR time scale due to phenyl rotation. No nuclear Overhauser effect (NOE) was observed between the 5-phenyl protons and those of L^-.

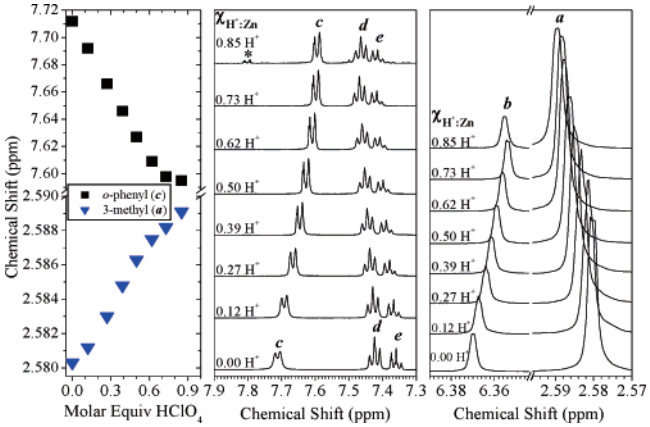

Figure 3. 500 MHz ^{1}H NMR spectra tracking the titration of [$Tp^{Ph,Me}$ZnOH] with $HClO_4$ in CD_3OD at 25 °C (middle and right panels). The asterisk indicates a resonance from partially dissociated $(Tp^{Ph,Me})^-$, which is reversed by subsequent titration with one of the bidentate ligands investigated in this study. The left panel shows single-proton titration curves derived from the dependences of proton *a* and *c* chemical shifts on the molar equivalents of H^+ added. The labeling scheme corresponds to that set forth in Scheme 1.

The other complexes exhibit chemical shift patterns analogous to that shown in Figure 2.

Protonation of [$Tp^{Ph,Me}$ZnOH]. Previous studies of [$Tp^{Ph,Me}$ZnOH] indicated that treatment with excess acid leads to demetalation of the complex and degradation of the $(Tp^{Ph,Me})^-$ ligand.[63] Given that reaction of this complex with the protic ligands, HL, investigated in this study yields water, the possibility of proton transfer from the ligand to hydroxide was considered. To address this possibility, it was necessary to elucidate the effects of protonating [$Tp^{Ph,Me}$ZnOH] on its ^{1}H NMR spectrum. This was accomplished by titration of [$Tp^{Ph,Me}$ZnOH] with $HClO_4$ in methanol-d_4. Figure 3 shows the effects of acid on the spectrum, which reveal three properties of this reaction that are consistent with the formation of $[Tp^{Ph,Me}Zn(OH_2)]^+$. First, chemical shifts of the $[Tp^{Ph,Me}Zn]^+$ moiety change upon treatment with substoichiometric amounts of acid. Only as the amount of acid approaches 1 equiv, do resonances attributable to partially dissociated $(Tp^{Ph,Me})^-$ (indicated by *) begin to appear in the spectrum. Second, the titration curves shown in the left panel of Figure 3 are consistent with a single-proton-transfer reaction. Finally, the simplicity of the spectrum and the constancy of the line widths at all points along the titration before the onset of $(Tp^{Ph,Me})^-$ dissociation suggest that addition of the proton does not break the symmetry of the molecule. Moreover, the acid induced partial dissociation of $(Tp^{Ph,Me})^-$ is reversible via subsequent addition of HL (*vide infra*). These observations are all consistent with protonation of the hydroxide ligand to yield the corresponding aqua complex, as shown in eq 2.

$$[Tp^{Ph,Me}ZnOH] + H^+ \rightleftharpoons [Tp^{Ph,Me}Zn(OH_2)]^+ \qquad (2)$$

Titration of [$Tp^{Ph,Me}$ZnOH] and $[Tp^{Ph,Me}Zn(OH_2)]^+$ by Protic Ligands (HL). The net reaction of [$Tp^{Ph,Me}$ZnOH]

(62) Bovey, F. A.; Jelinski, L.; Mirau, P. A. *Nuclear Magnetic Resonance Spectroscopy*, 2nd ed.; Academic Press: San Diego, CA, 1987.
(63) Alsfasser, R.; Vahrenkamp, H. *Chem. Ber.* **1993**, *126*, 695−701.

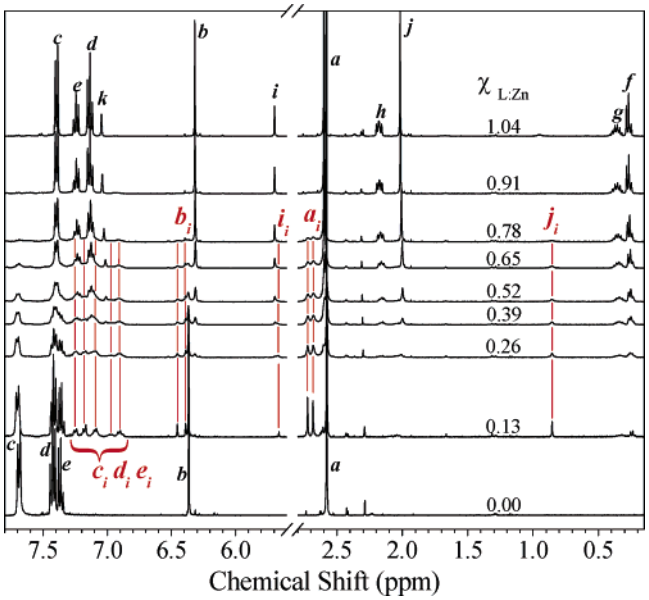

Figure 4. 500 MHz ^{1}H NMR spectra that track the titration of [Tp^{Ph,Me}ZnOH] with 5-Me-4-ImHPr in CD_3OD at 25 °C. The red lines and labels indicate resonances corresponding to intermediate complexes that appear upon the first addition of 5-Me-4-ImHPr and disappear as L/Zn approaches 1:1. The labeling scheme corresponds to that set forth in Scheme 1.

with HL, where HL is 2-ImHPr, 4-ImHPr, or 5-Me-4-ImHPr, involves the neutralization of OH^- by H^+ and the coordination of L^- to the Zn^{2+} as shown in eq 3. Upon titration of

$$[Tp^{Ph,Me}ZnOH] + HL \rightleftharpoons [Tp^{Ph,Me}ZnL] + H_2O \qquad (3)$$

[Tp^{Ph,Me}ZnOH] in methanol-d_4 with HL at 25 °C, the ^{1}H NMR spectra changed systematically from that of [Tp^{Ph,Me}ZnOH] to those of the respective final products. The final spectra were identical to those obtained from solutions of the pure isolated complexes. The spectra obtained during titrations of [Tp^{Ph,Me}ZnOH] with 5-Me-4-ImHPr (Figure 4) and 4-ImHPr (Figure S1 of the Supporting Information) are similar. The spectra of solutions containing substoichiometric amounts of 5-Me-4-ImHPr and 4-ImHPr contain resonances of intermediate species, which are marked by red vertical lines in Figures 4 and S1. The spectra from the 4-ImHPr titration contain one set of resonances attributable to a single intermediate. Those from the 5-Me-4-ImHPr titration contain a second set, consistent with two intermediates. As the stoichiometry approached HL/Zn = 1:1, these resonances along with their counterparts in the [Tp^{Ph,Me}ZnOH] and [Tp^{Ph,Me}Zn(5-Me-4-ImPr)] spectra broadened due to site exchange and ultimately gave way to the sharp resonances of the (5-Me-4-ImPr)$^-$ and (4-ImPr)$^-$ chelates, as they became the dominant products. This site exchange is consistent with competition among multiple ligands for the two coordination sites on the [Tp^{Ph,Me}Zn]$^+$ moiety. However, the spectral resolution of resonances attributed to starting material, intermediates, and final product at substoichiometric HL concentrations indicates that their interconversions are slow on the NMR time scale. No resonances attributable to reaction intermediates appear during the 2-ImHPr titration.

Insight into the mechanistic aspects of these ligand substitution reactions is gained by comparing the evolution

Scheme 2

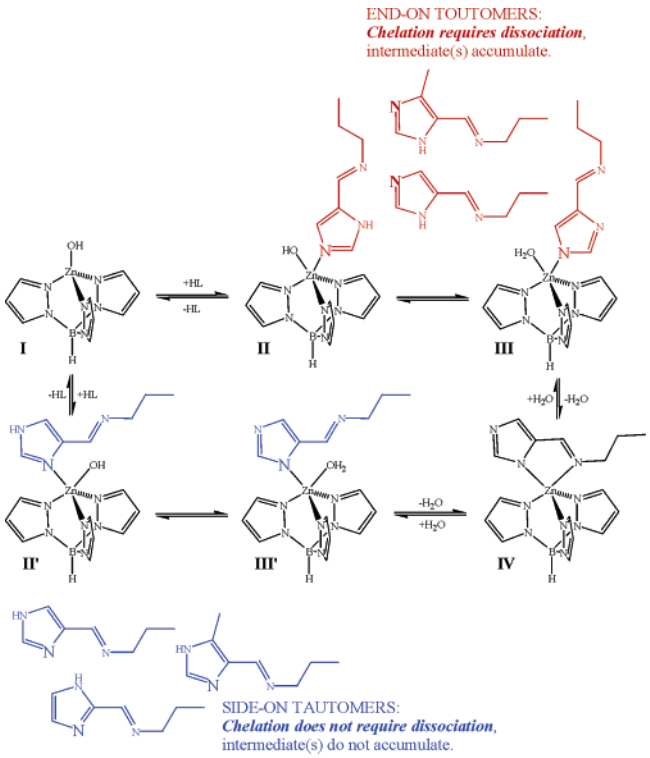

of spectral features during the 5-Me-4-ImHPr, 4-ImHPr, and 2-ImHPr titrations. Two intermediate complexes appear during the 5-Me-4-ImHPr titration (Figure 4), whereas only one is observed for 4-ImHPr (Figure S1). On the basis of this nuance, one could argue for a stepwise mechanism, as illustrated in Scheme 2, involving monodentate HL (II and II′ in Scheme 2) and L^- (III and III′ in Scheme 2) that are coordinated through one of the imidazolyl nitrogen atoms. Although binding through the acyclic imine N atom cannot be discounted, we suggest here that the imidazolyl N atoms are most likely to bind because of their greater basicities. In this model, the two "end-on" mixed ligand intermediates (II *and* III in Scheme 2) are populated about equally in the 5-Me-4-ImHPr titration, whereas only one (II *or* III in Scheme 2) builds up to detectable levels in the 4-ImHPr titration. Alternatively, the intermediates for 4-ImHPr could be in rapid exchange, thereby giving rise to average intermediate resonances. In either case, the detectable buildup of the end-on intermediates is easily rationalized because the formation of the final ZBG chelates requires the dissociation of both the water molecule and the monodentate ligand.

The 2-ImHPr ligand is distinct from 5-Me-4-ImHPr and 4-ImHPr in that its imidazole N atoms are chemically equivalent in its deprotonated form, (2-ImPr)$^-$. Thus, regardless of which imidazole N atom is coordinated, this ligand can form a five-membered zinc chelate without dissociation of the imidazolate ligand. This structural difference is manifested in distinct solution behavior, as shown by the NMR spectra in Figure 5. Specifically, in contrast to the cases of the 5-Me-4-ImHPr and 4-ImHPr titrations, buildup of mixed ligand intermediates was not observed in the 2-ImHPr titration. Similar behavior was observed for the titration of

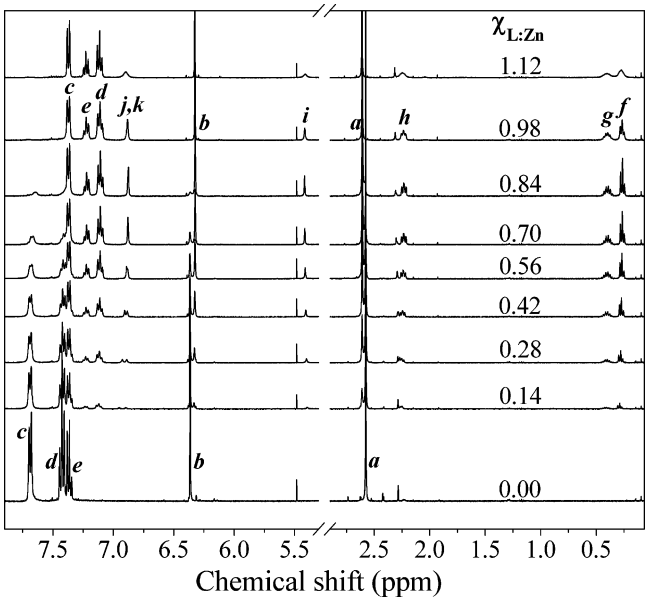

Figure 5. 500 MHz ^{1}H NMR spectra that track the titration of [Tp^{Ph,Me}ZnOH] with 2-ImHPr in CD_3OD at 25 °C. The labeling scheme corresponds to that set forth in Scheme 1.

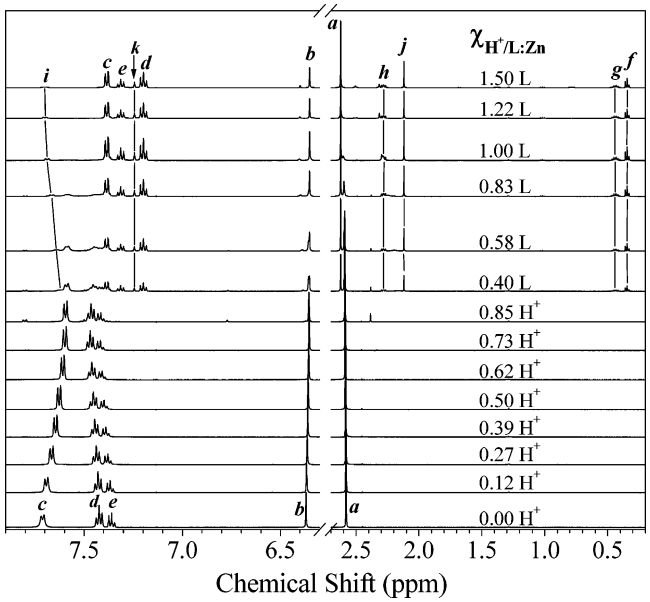

Figure 6. 500 MHz ^{1}H NMR spectra showing the effects of sequential titration of [Tp^{Ph,Me}ZnOH] with $HClO_4$ and 5-Me-4-ImHPr in CD_3OD at 25 °C. The solid lines indicate 5-Me-4-ImHPr resonances. Note that once the OH^- ligand is protonated, there is no evidence of the intermediate seen in Figure 4. The labeling scheme corresponds to that set forth in Scheme 1.

[Tp^{Ph,Me}ZnOH] with 2-HOPhPr, as shown in Figure S2 of the Supporting Information. The 2-ImHPr case is similar to that described above for the side-on mixed ligand adducts of 5-Me-4-ImHPr and 4-ImHPr in that formation of the chelate does not require dissociation of the monodentate 2-ImHPr ligand. Thus, water dissociation is likely the major contributor to the kinetic barrier to chelate formation. Due to the relatively long time scale of the NMR experiment, the data presented here cannot distinguish between the possibilities of a concerted ligand substitution and rapid but sequential hydroxide protonation by monodentate 2-ImHPr or 2-HOPhPr (or by side-on monodentate 5-Me-4-ImHPr and 4-ImHPr), water dissociation, and chelation.

If [Tp^{Ph,Me}Zn(OH$_2$)]$^+$ is prepared by titration with $HClO_4$ and subsequently titrated with 5-Me-4-ImHPr, as shown in Figure 6, the resonances of the intermediate complex are not observed. Rather, there appears to be direct conversion of [Tp^{Ph,Me}Zn(OH$_2$)]$^+$ to [Tp^{Ph,Me}Zn(5-Me-4-ImHPr)]. Thus, a five-coordinate intermediate comprising aqua and monodenate 5-Me-4-ImHPr or 5-Me-4-ImPr$^-$ ligands is not sufficiently stable to exist at detectable concentrations. This observation suggests that once the hydroxide ligand of [Tp^{Ph,Me}ZnOH] is protonated, it readily dissociates or is readily displaced by the bidentate ligand.

Titration of [Tp^{Ph,Me}ZnOH] and [Tp^{Ph,Me}Zn(OH$_2$)]$^+$ by Aprotic Ligands. While the OH^- ligand is readily displaced by the anionic L^- ligands discussed above and by other anions, such as halides, CO_3^{2-} (from CO_2), and alkoxides,[2] the displacement of OH^- by neutral ligands appears less favorable. The ^{1}H NMR spectral changes induced by titration of [Tp^{Ph,Me}ZnOH] with the neutral ligands (L′), 2-TaPr and 1-Me-2-ImPr, were distinct from those shown in Figures 4−6. The bottom seven spectra of Figure 7 show the changes that occur upon titration of [Tp^{Ph,Me}ZnOH] with 2-TaPr in methanol-d_4. The features of these spectra suggest that 2-TaPr binds to Zn, albeit less strongly than its anionic imidazolyl

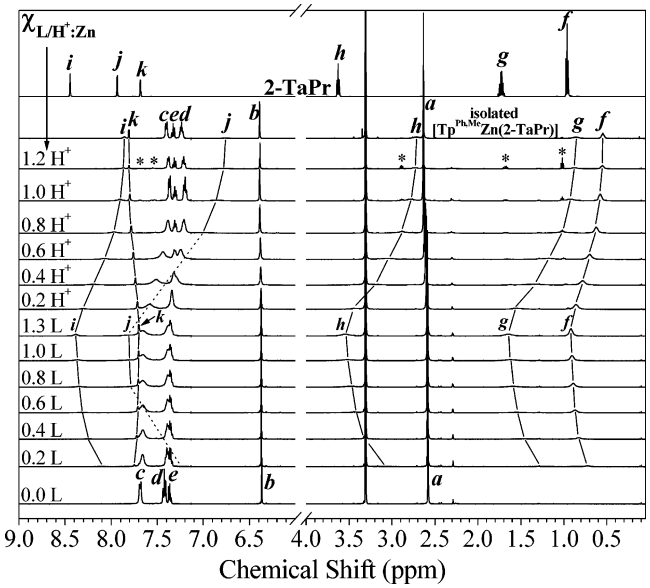

Figure 7. 500 MHz ^{1}H NMR spectra showing the effects of sequential titration of [Tp^{Ph,Me}ZnOH] with the aprotic ligand 2-TaPr, followed by $HClO_4$, at 25 °C. Solid lines indicate the chemical shift behavior of the 2-TaPr resonances. The asterisks indicate resonances consistent with monodentate thiazole-bound 2-TaPr due to protonation of the ligand by a 20% molar excess of acid in the top spectrum. The labeling scheme corresponds to that set forth in Scheme 1.

counterparts, and that its protons undergo rapid site exchange between their bound and free states. The exchange is apparent from the single set of ligand resonances, whose line widths and chemical shifts depend on its concentration at each point in the titration. All except proton *k* become rather broad due to substantial ring current induced chemical shift differences between the free and bound 2-TaPr ligand. The resonance corresponding to proton *k* remains relatively sharp because its chemical shift only changes by 0.13 ppm upon binding

to the zinc complex. This insensitivity is attributed to the nearly offsetting effects of coordination to Zn^{2+} (deshielding) and the ring current shift due to the 3-phenyl groups of the $(Tp^{Ph,Me})^-$ ligand (shielding). With increasing concentrations of 2-TaPr, the chemical shifts of its exchange-broadened resonances approach those of the free ligand. This trend provides a clear basis for the assignment of the bound ligand resonances. Given the breadth and chemical shifts of the 2-TaPr resonances throughout the titration, neither the coordination number of the complex nor the denticity of 2-TaPr is clear from these spectra. This reaction is distinct from those described above for the protic ligands, as the formation and liberation of a water ligand cannot contribute to the driving force for the formation of $[Tp^{Ph,Me}Zn(2\text{-}TaPr)]^+$. In the absence of a proton source, 2-TaPr can either displace the OH^- ligand to yield a pentacoordinate cationic zinc complex, as shown in eq 4, or add to the complex to generate a neutral penta- or hexacoordinate complex as per eq 5. Thus, the free energy of formation of an aprotic ligand complex must pay either the price of charge separation that must accompany the dissociation of the hydroxide ligand to form a cationic pentacoordinate complex, as in (4), or the steric cost of the interaction with the 3-phenyl groups of $(Tp^{Ph,Me})^-$ in a hexacoordinate complex, as in (5).

$$[Tp^{Ph,Me}ZnOH] + L' \rightleftharpoons [Tp^{Ph,Me}Zn(L')]^+ + OH^- \quad (4)$$

$$[Tp^{Ph,Me}ZnOH] + L' \rightleftharpoons [Tp^{Ph,Me}Zn(OH)(L')] \quad (5)$$

The top spectra in Figure 7 show that, with sequential additions of $HClO_4$, the 2-TaPr resonances, except for *k*, shift upfield toward their chemical shifts in the spectrum of the isolated product, $[Tp^{Ph,Me}Zn(L')](ClO_4)$. This behavior is consistent with acid causing a greater fraction of the 2-TaPr ligand to be bound, although the bound and free 2-TaPr still exchange rapidly. Therefore, coordination of 2-TaPr can be driven by the introduction of H^+, which reacts with the OH^- ligand to yield a water molecule, as shown in eq 6. Similar behavior is observed for the aprotic 1-Me-2-ImPr ligand (Figure S3 of the Supporting Information).

$$[Tp^{Ph,Me}ZnOH] + L' + H^+ \rightleftharpoons [Tp^{Ph,Me}Zn(L')]^+ + H_2O \quad (6)$$

The breadth and continued upfield shift of the 2-TaPr resonances suggested that the complex was not saturated and that 2-TaPr was in rapid exchange between its free, bound, and probably partially bound forms. It is also possible that sulfur coordination is involved in these exhange dynamics. However, the NMR data neither support nor refute this possibility. In an attempt to determine the actual chemical shifts of the 2-TaPr complex, we prepared $[Tp^{Ph,Me}Zn(OH_2)]^+$ in situ by titrating $[Tp^{Ph,Me}ZnOH]$ with $HClO_4$, as shown in the bottom five spectra of Figure 8. Subsequent titration with 2-TaPr revealed a new set of resonances in the spectra treated with substoichiometric amounts of ligand. These resonances, which appear in the spectrum after addition of 0.16 equiv of 2-TaPr (Figure 8), were further upfield than those of the isolated $[Tp^{Ph,Me}Zn(2\text{-}TaPr)]^+$ complex (Figure 7). With further additions of 2-TaPr, its resonances shift toward their

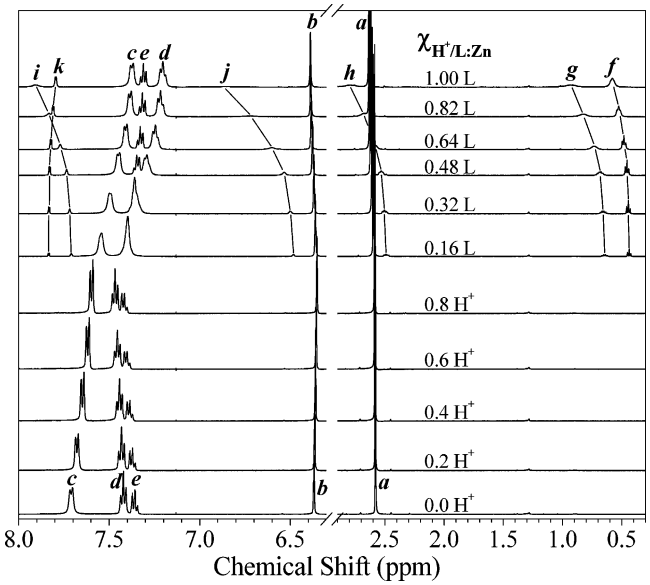

Figure 8. 500 MHz ^1H NMR spectra showing the effects of sequential titration of $[Tp^{Ph,Me}ZnOH]$ with $HClO_4$, followed by the aprotic ligand 2-TaPr, at 25 °C. Solid lines indicate the chemical shift behavior of the 2-TaPr resonances as water is displaced from the zinc center. The labeling scheme corresponds to that set forth in Scheme 1.

positions in the spectra of the isolated complex (and of the free ligand, Figure 7) as the fraction of the Zn-bound ligand diminishes. Additionally, as the rate of exchange increases with increasing 2-TaPr concentration, the resonances are seen to broaden.

The spectra in Figure 7 are consistent with the speciation of the $[Tp^{Ph,Me}Zn]^+$ center shown in eq 7 when $[Tp^{Ph,Me}ZnOH]$ is titrated first with the neutral bidentate ligand, L′, and then with acid. Equation 8 represents the course of events suggested by the spectra in Figure 8, which show titration of $[Tp^{Ph,Me}ZnOH]$ with acid followed by addition of L′.

$$[Tp^{Ph,Me}ZnOH] \underset{-L'}{\overset{+L'}{\rightleftharpoons}} [Tp^{Ph,Me}Zn(OH)(L')] \underset{-H^+}{\overset{+H^+}{\rightleftharpoons}} [Tp^{Ph,Me}Zn(L')]^+ + H_2O \quad (7)$$

$$[Tp^{Ph,Me}ZnOH] \underset{-H^+}{\overset{+H^+}{\rightleftharpoons}} [Tp^{Ph,Me}Zn(OH_2)]^+ \underset{-L'}{\overset{+L'}{\rightleftharpoons}} [Tp^{Ph,Me}Zn(L')]^+ + H_2O \quad (8)$$

Relevance to the Inhibition of Metalloproteases. Tris histidyl coordination to the catalytic zinc center is a hallmark of the MMPs and ADAMs. Moreover, like the many $[Tp^{Ph,Me}Zn(L)]$[64] structures, crystal structures of uninhibited MMP catalytic domains[12,65] indicate $N_{His}-Zn-N_{His}$ angles that are typically less than the 109.5° of tetrahedrally coordinated zinc. In addition to the three endogenous His ligands, the activated resting metalloproteases are thought to have a hydrogen-bonded water[66] or a hydroxide[67] ligand coordinated

(64) Trofimenko, S. *Scorpionates: The Coordination Chemistry of polypyrazolylborate Ligands*; Imperial College Press: London, 1999.
(65) Dhanaraj, V.; Williams, M. G.; Ye, Q.-Z.; Molina, F.; Johnson, L. L.; Ortwine, D. F.; Pavlovsky, A.; Rubin, J. R.; Skeean, R. W.; White, A. D.; Humblet, C.; Hupe, D. J.; Blundell, T. L. *Croat. Chem. Acta* **1999**, *72*, 575−591. Moy, F. J.; Chanda, P. K.; Cosmi, S.; Pisano, M. R.; Urbano, C.; Wilhelm, J.; Powers, R. *Biochemistry* **1998**, *37*, 1495−1504.

to the catalytic zinc center. In the currently accepted MMP mechanism, this water molecule adds across the scissile peptide bond during the hydrolysis reactions catalyzed by these enzymes.[68] The most potent inhibitors to date have contained ZBGs that disrupt access of the substrate to the catalytic water molecule by forming stable four-, five-, or six-coordinate[3,9−26] zinc complexes. Thus, insofar as the OH^- ligand of [$Tp^{Ph,Me}$ZnOH] mimics the resting enzyme with the catalytic water molecule bound to the active site zinc center, studies of its displacement by inhibitory ZBGs can provide insight into the structural and electronic factors that determine the thermodynamic and kinetic stabilities of inhibited MMPs.

Mechanistic studies of other metalloproteases have provided compelling evidence for a hyperacidic catalytic Zn−OH_2 center with p$K_a \simeq 5$.[67] On that basis, the solvent oxygen in the enzyme resting state would be bound to zinc in the form of a hydroxide ligand at physiological pH. Dissociation of that solvent oxygen is promoted by a proton source which, in the case of a zinc-binding inhibitor, could be the zinc-binding or chelating group. Thus, the acidity of the bound water ligand in the model complex investigated here may be quite relevant to the catalytic chemistry of zinc-dependent metalloproteases. Moreover, the courses of events shown in eqs 7 and 8 that culminate in the corresponding ZBG complexes very likely mimic their analogous steps in the displacement of catalytic water by zinc-binding inhibitors in the enzymes.

The results of this study suggest that, in addition to the energy yield from the formation of five-membered chelates, the blocked catalytic zinc center is likely to be thermodynamically and kinetically stabilized by ZBGs that form relatively acidic zinc complexes. A propensity for proton donation contributes to inhibition by two related means. First, it promotes dissociation of the catalytic solvent water from zinc by diminishing the negative charge on the coordinated oxygen atom. Second, it yields an active site zinc complex bearing only a single positive charge. This undoubtedly diminishes its Lewis acidity and, consequently, its catalytic efficacy, even if a water molecule can still coordinate. Recent computational work suggests that, in the enzyme catalytic sites, protic nitrogen-, oxygen-, and sulfur-based zinc-binding groups form sufficiently acidic zinc complexes that they transfer a proton to the side chain of the invariant active site glutamate, thereby forming inhibited active site complexes bearing a single positive charge.[59] However, whether the tendency of a ZBG toward proton donation results in partial (H-bond donation by the ZBG) or complete proton transfer within the active site, a protic ZBG opens the possibility of establishing or reorganizing one or more nonbonded interactions between the bound ZBG and the enzyme active site, while diminishing the positive charge and, consequently, the Lewis acidity of the zinc center, upon which the catalytic activity of the active site depends. The results of this study are consistent with these effects contributing synergistically to the overall stability of the inhibited enzymes.

Conclusion

Variously substituted hydridotris(pyrazole-1-yl)borate complexes of Zn^{2+} have been investigated extensively for their structural similarity to the catalytic centers in several classes of zinc-dependent enzymes.[2] As such, they serve as platforms for investigating the coordination chemistry between the enzyme active sites and competitive inhibitors of the enzymes, and several reports on the interactions of these model compounds with zinc-binding ligands that exhibit inhibitory activity have also appeared.[30−35] In this report, we have presented structural and spectroscopic results from a model complex study that provides insight into the interactions between the catalytic zinc centers of MMPs and ADAMs and bidentate chelating ligands known to exhibit moderate inhibition of MMPs. Single-crystal X-ray structures revealed that the protic imidazolyl-based ligands coordinate as anions with the elimination of a water molecule to give neutral complexes. The corresponding ^{1}H NMR titrations show that these chelates form with large stability constants, as no detectable [$Tp^{Ph,Me}$ZnOH] remains after addition of 1 equiv of the ligands. In contrast, the aprotic thiazolyl- and 1-methyl-2-imidazolyl-based ligands form less stable complexes than their protic counterparts because of their inability to supply a proton for the elimination of a water molecule. Complete chelation of the zinc center by these ligands requires excess ligand, consistent with the lower stability of the complex. Moreover, the aprotic ligand complexes are more dynamic, indicating that they are also kinetically less stable toward ligand exchange under equilibrium conditions. These results provide one possible explanation of why hydroxamic and carboxylic acids have proven to be such effective zinc-binding groups. Moreover, this study suggests that protic ZBGs are good design targets for the next generation of MMP and ADAM inhibitors.

Acknowledgment. This work was supported by NCRR P20RR15566 (K.R.R.), AHA 0550089Z (K.R.R.), AHA 0430009N (S.M.C.), and the Rebecca and John Moores UCSD Cancer Center (S.M.C.).

Supporting Information Available: Crystallographic information files for [$Tp^{Ph,Me}$Zn(5-Me-4-ImPr)]·C_6H_6, [$Tp^{Ph,Me}$Zn(2-ImPr)]·C_6H_6, and [$Tp^{Ph,Me}$Zn(2-HOPhPr)](ClO_4) along with Figures S1, S2, S3, and S4 showing the ^{1}H NMR spectra from the titrations of [$Tp^{Ph,Me}$ZnOH] by 4-ImHPr, 4-ImHPr/$HClO_4$, 2-HOPhPr, and 1-Me-2-ImPr, respectively. This material is available free of charge via the Internet at http://pubs.acs.org.

IC050723P

(66) Willenbrock, F.; Knight, C. G.; Murphy, G.; Phillips, I. R.; Brocklehurst, K. *Biochemistry* **1995**, *34*, 12012−12018.
(67) Mock, W. L.; Aksamawati, M. *Biochem. J.* **1994**, *302*, 57−68. Mock, W. L.; Stanford, D. J. *Biochemistry* **1996**, *35*, 7369−7377. Mock, W. L.; Cheng, H. *Biochemistry* **2000**, *39*, 13945−13952.
(68) Harrison, R. K.; Chang, B.; Niedzwiecki, L.; Stein, R. L. *Biochemistry* **1992**, *31*, 10757−10762. Izquierdo-Martin, M.; Stein, R. L. *J. Am. Chem. Soc.* **1992**, *114*, 325−331. Lovejoy, B.; Hassell, A. M.; Luther, M. A.; Weigl, D.; Jordan, S. R. *Biochemistry* **1994**, *33*, 8207−8217. Pelmenschikov, V.; Siegbahn, P. E. M. *Inorg. Chem.* **2002**, *41*, 5659−5666.